UNIVERSITY OF CAMBRIDGE
Department of Engineering

Analysis of Tremie Concrete Behaviour During Bleeding

Author Name: **Jin Zheng**
Supervisor: **Dr. Giovanna Biscontin**
Date: **28 May 2019**

I hereby declare that, except where specifically indicated, the work submitted herin is my own original work.

Signed ___________ *date* 28 May 2019

Analysis of Tremie Concrete Behaviour During Bleeding

Final Report

Jin Zheng (jz410)

Supervisor: Dr. Giovanna Biscontin

Department of Engineering

University of Cambridge

I hereby declare that, except where specifically indicated, the work submitted herein is my own original work.

Signed:

Date: 28 May 2019

Homerton College

May 2019

Acknowledgements

The author gratefully acknowledges Dr. Giovanna Biscontin, Mr. Christopher Wilkes, Mr. Duncan Nicholson and Ms. Irina Shmeleva for valuable help and suggestions, and Arup for the support of this project.

Analysis of Tremie Concrete Behaviour During Bleeding
Technical Abstract

Jin Zheng (Homerton College)
Supervisor: Dr. Giovanna Biscontin

Bleeding of tremie concrete in deep foundations is becoming a concern on construction sites, due to the need for large amounts in deep foundations and high workability from the application of superplasticiser. Bleeding of tremie concrete can cause or aggravate channelling, segregation, mattressing and bleed water accumulation around aggregate and reinforcement. These imperfections can lead to further non-uniform strength distribution, reinforcement corrosion and other durability problems. Moreover, the current on-site bleeding test is not compulsory and lasts for two hours, yet it only has a single limit on the average bleeding rate. As a result, a better understanding of the bleeding mechanism of modern tremie concrete can help the industry to improve the current site test and minimise the adverse impacts of bleeding. This project was consequently proposed to analyse the tremie concrete behaviour during bleeding, along with objectives to confirm a proposed bleeding model based on the literature review, and to provide recommendations for improving the site test and reducing excessive bleeding based on the analysis of results from the developed experiment.

There are two main models employed to explain the bleeding mechanism: sedimentation and consolidation. Bleeding rate and bleeding capacity are the two factors influencing the bleeding phenomenon. Due to the size and boundary conditions of deep foundations, the one-dimensional self-weight consolidation model was suggested to describe the bleeding mechanism of modern tremie concrete. Theoretical solutions of one-dimensional self-weight consolidation were then derived from Terzaghi's equation.

Since the addition of chemical admixtures and the high content of fine particles can influence the measurement of surface subsidence, the proposed model was decided to be confirmed by the pore pressure measurement which is the driver of the consolidation mechanism. Nonetheless, no previous study confirms the bleeding of modern concrete by examining pore pressure variations.

The Pore Pressure Cylinder (PPC) test was accordingly designed to determine pore pressure variations during bleeding. The PPC apparatus was set up and preliminarily tested in the Michaelmas term. In the preliminary tests, a reference mix design and five other extreme cases of bleeding (by modifying the water-binder ratio, and amount of fine sand and superplasticiser) were used to examine the validity, reliability and repeatability of the PPC test. The test results showed that the PPC test was suitable for further experiments to validate the proposed bleeding model.

Moreover, the PPC test was also performed on site to check its site practicality and the quality of laboratory tremie concrete. Regardless of the noticeable noise on site, the PPC test produced analysable results. The site test data also improved the preparation of laboratory tremie concrete by adding a pre-saturation stage, leading to the bleeding behaviour of the reference mix design becoming similar

to the tremie concrete used on site.

Five repeated experiments of the reference mix design were performed to compare with the proposed bleeding model. The experimental results were to some extent close to the theoretical solutions of the model, but not all repeated results aligned closely with those solutions. It was observed that there might be other reactions (i.e. setting, hydration, etc.) dominating tremie concrete behaviour after around 15 minutes, as the pore pressure dissipation rate (thus, the bleeding rate) was significantly reduced. Nevertheless, the comparison of results over the initial 15 minutes still showed discrepancies between experimental results and theoretical solutions.

The experimental data and observations indicated that the pre-saturation stage can increase the initial bleeding rate and worsen bleeding. Since the bleeding capacity is related to the designed water content that should be re-absorbed by tremie concrete at last, it can be concluded that the initial bleeding rate probably dominates the overall bleeding, and more attention should be paid to it in the future research.

Another attempt was also made to study the effect of the specific surface area on bleeding. Four additional experiments (pure cement paste, cement paste with fine sand, reference mix with less fine sand, and reference mix with more fine sand) were carried out. The decrease of the specific surface area generally increased the bleeding rate. The experimental data of modern cement pastes (used in this project) were similar to the results reported in a recent study, but not to an earlier study with traditional cement pastes. This may indicate the difference between the modern and traditional cement-based materials.

Furthermore, the proposed bleeding model was also examined with the results from the specific surface area tests. For the first 15 minutes, theoretical solutions were found to be closer to the experimental results from the specific surface area tests than those from repetitions of the reference mix design. This may indicate that the data from repetitions of the reference mix design were not accurate enough, and this might be caused by the preparation of laboratory tremie concrete. Therefore, further work is required to improve the consistency of the prepared tremie concrete. Future repetitions should also include parallel standard tests to check the consistency of tremie concrete.

Overall, the PPC test was proved to be applicable to analyse the bleeding of tremie concrete. An approximate range of bleeding rates can be deduced for a certain type of tremie concrete based on repetitions of the PPC test. Moreover, there is potential for using the PPC test on site to improve the robustness of the site bleeding test while reducing its duration. However, revisions are required for the proposed one-dimensional self-weight consolidation model, along with improvements on the production of laboratory tremie concrete. The pre-saturation stage and the amount of fine sand can affect bleeding of tremie concrete, but any modifications should take account of their impacts on other tremie concrete properties.

Table of contents

1 Introduction

1.1 Project Motivation

Tremie concrete is a special type of Self-Compacting Concrete (SCC) used in deep foundation construction. It is placed by tremie pipes under submerged conditions, as shown in Figure 1.1 [1]. Bleeding describes the phenomenon when water gradually appears on the top of freshly mixed concrete after placement [2]. Figure 1.2 shows bleeding in one of the experiments performed in this project.

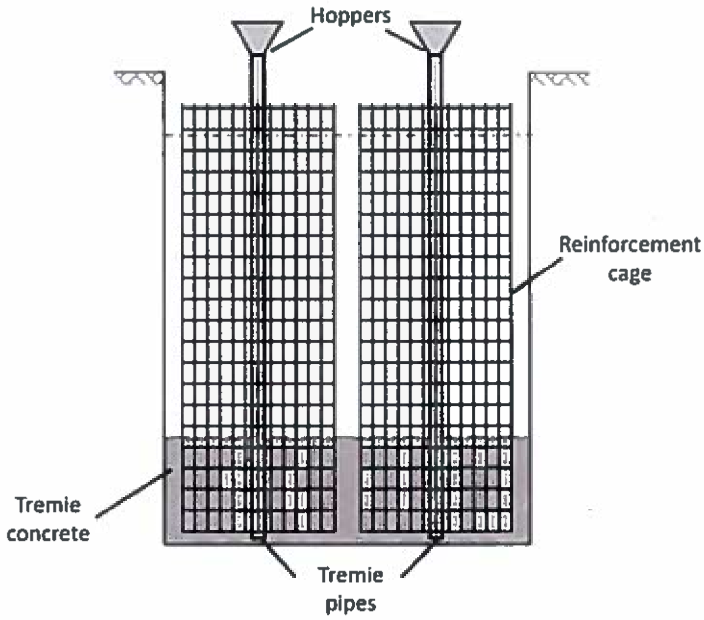

Figure 1.1: Tremie concrete placing method [1]

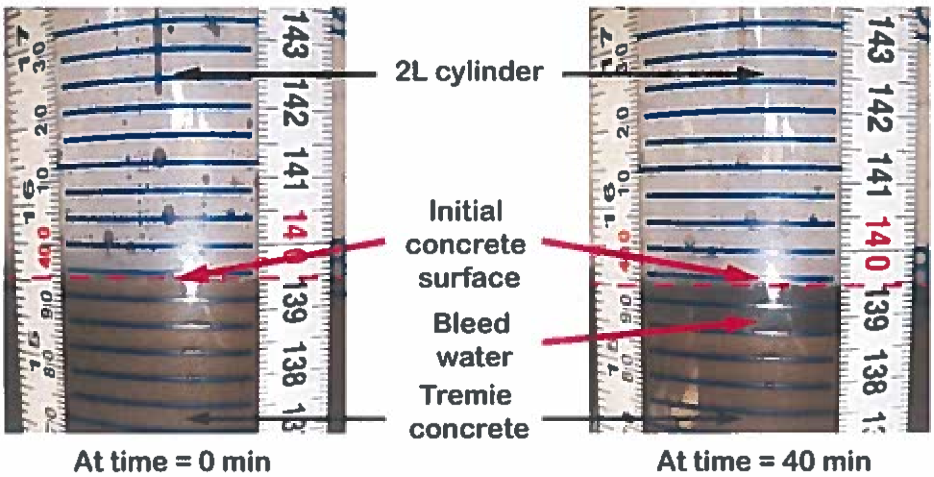

Figure 1.2: Observation of bleeding after 40 minutes of tremie concrete placement

Bleeding is generally not a major concern for normal concrete in thin slabs and walls [3]. For deep foundations and retaining walls, however, bleeding of tremie concrete is becoming a concern on construction sites [1, 3, 4]. There are two main reasons for such a concern [1, 5]:

1. The foundation size requires a considerable amount of tremie concrete;

2. The addition of superplasticiser enables tremie concrete to have a much longer workability period before setting than under normal conditions.

Figures 1.3 and 1.4 show the grout volcano and aggregate-deficient zone in deep foundations observed in recent research, as an excessive amount of bleed water was rapidly extruded to the top of tremie concrete [4].

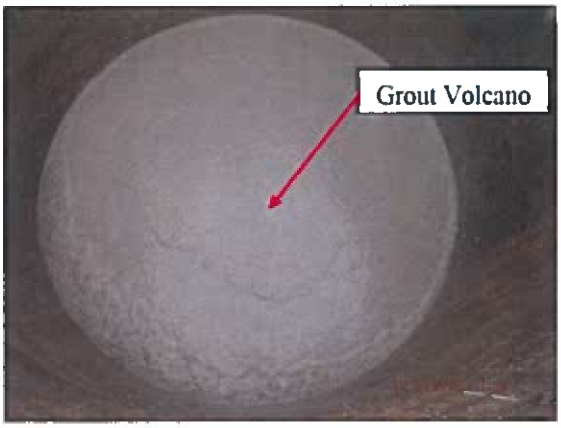

Figure 1.3: Grout volcano [4]

Figure 1.4: Aggregate-deficient zone [4]

Bleeding of tremie concrete can cause or aggravate at least four effects in deep foundations and retaining walls. First, bleeding aggravates the segregation of materials in a structure [1, 3]. Research shows that the decrease in density from the bottom to the top of the pile (due to segregation) leads to a decrease in strength in the same direction [1, 3]. The reduction in strength at the top of the pile, therefore, may cause the performance to be inconsistent with design expectations [4]. The graphical log in Figure 1.5 examines the segregation of tremie concrete by measuring the density of different pile samples. It can be seen that aggregate-deficient (grout and mortar) zones extend up to 4 meters below the cut-off level [4].

Second, as water seeps to the top of the placement, channels form along the vertical reinforcement and on the surface of the structure [1, 2]. Since bleed channels can have considerable sizes, issues can arise with regards to the durability of the structure [1, 3, 4]. Figure 1.6 shows the channelling on the surface of a retaining wall [6].

Third, the paste-aggregate and paste-reinforcement bond strengths are reduced when bleed water accumulates and forms voids around large aggregate and reinforcement, (Figure 1.7) [3, 6]. The reduction in bond strengths reduces the overall structure strength. Excessive water collection and void formation around reinforcement can also trigger corrosion [3].

Finally, bleed channels can exaggerate the vertical mattressing effect (Figure 1.8). The section plot of the mattressing effect in Figure 1.9 illustrates how tremie concrete is trapped in the shadow of the reinforcement during mattressing. Vertical bleed channels can increase the extent of mattressing by resisting the flow of tremie concrete around reinforcement [1]. Insufficient covers in a structure can lead to durability and bearing capacity problems [1].

Nevertheless, current site tests of bleeding is not compulsory and lasts for two hours [7, 8]; a significantly long time for a site to wait. The measurement of bleed water is also susceptible to the quality of workmanship, as bleed water is collected manually. Guidelines only provide an upper limit of 0.1 ml/min for the bleeding test of tremie concrete, without clearly explaining how this value (0.1 ml/min) relates to the actual performance [1].

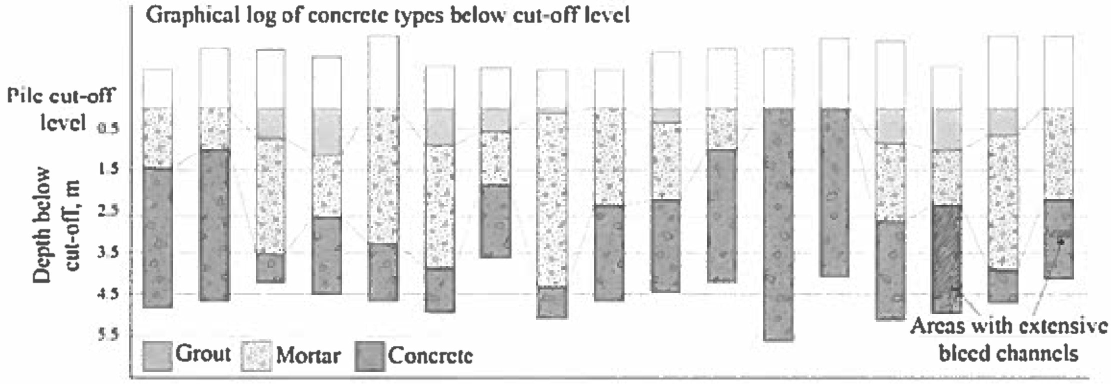

Figure 1.5: Segregation on the top of different piles [4]

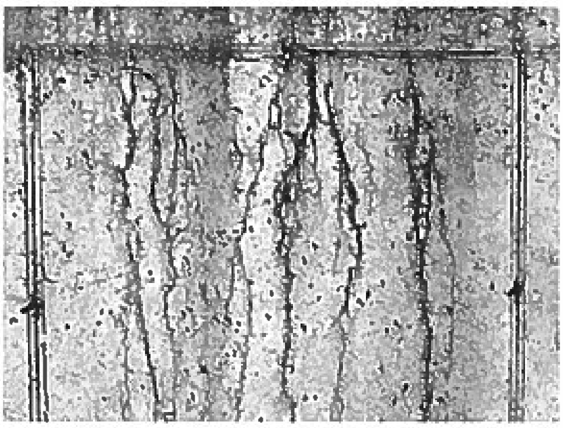

Figure 1.6: Channelling effect (retaining wall width: 2-3 m)[6]

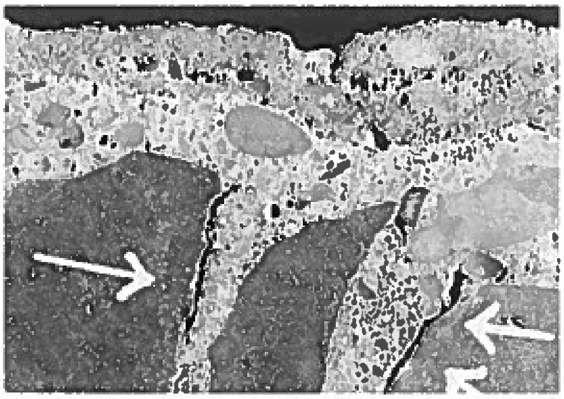

Figure 1.7: Voids formation (aggregate size: 5-10 mm) [6]

Figure 1.8: Mattressing (retaining wall width: 1-2 m)[1]

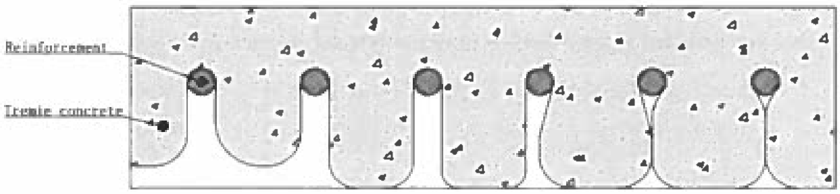

Figure 1.9: Section plot of the vertical mattressing (section width: 0.5 m)

1.2 Project Objectives

This project stemmed from the concern about excessive bleeding in deep foundations and the impracticality of current site tests for tremie concrete. As a result, a better understanding of the bleeding mechanism of tremie concrete can not only improve and validate current site tests, but also reduce its detrimental effects from mixing to final placement.

Accordingly, the objectives of this project were to:

1. Summarise existing concepts and models of bleeding (of cement-based materials);
2. Propose a model of tremie concrete bleeding;
3. Derive theoretical solutions for the proposed model;
4. Develop an experiment to confirm the derived theoretical solutions;
5. Qualify the bleeding effect with the new experiment;
6. Provide recommendations for improving the site test and reducing excessive bleeding from the experimental results.

As shown in the following chapter, the proposed bleeding mechanism is one-dimensional self-weight consolidation. Consequently, it was determined to compare the pore pressure variations of freshly placed tremie concrete with the theoretical solutions of the proposed mechanism derived from Terzaghi's equation.

In the Michaelmas term, the Pore Pressure Cylinder (PPC) experiment for measuring the bottom pore pressure was set up and preliminarily tested. In the Lent term, the theoretical results predicted by the one-dimensional self-weight consolidation theory were calculated and compared with repeated PPC tests of a reference mix design. Meanwhile, the mixing method was upgraded by comparing the PPC site test data with the laboratory data. Attempts were also made to investigate the effect of the specific surface area on bleeding. A Gantt chart for this project is shown in Figure 1.10. Details of the proposed theory, apparatus, experimental and theorical results, and further recommendations are provided in following chapters.

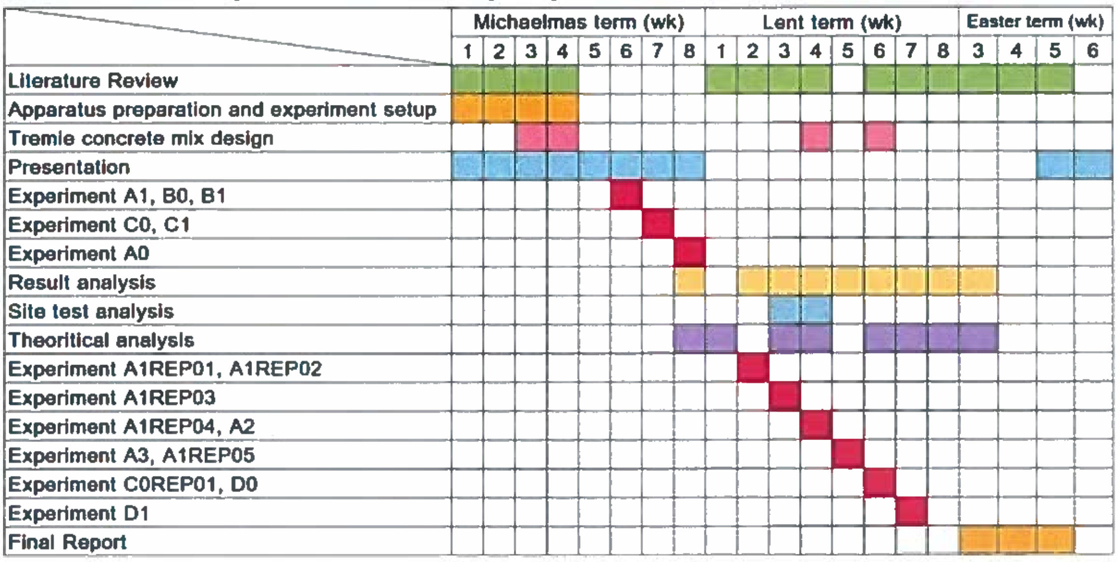

Figure 1.10: Gantt chart for the project

2 Literature Review and Theory

This chapter summarises concepts, terminologies, models, experiments and methods relevant to bleeding of cement-based materials. Due to recent developments in cement and concrete technologies (especially for tremie concrete), limitations of previous studies and the opportunity of further research are also discussed in this chapter.

2.1 Bleeding Concepts and Terminologies

In 1968, Powers argued that bleeding of cement-based materials (i.e. cement paste, concrete, etc.) was a consequence of settlement under their self-weight [2]. According to this argument, the freshl cement-based material is an unstable suspension of particles immediately after placement. Because of the difference in density between water and particles, the particles start to move downwards. This results in an upward migration of water, most of which accumulates on the surface of the placement, while maintaining a constant total volume. This gradual accumulation of water is called bleeding, and the extruded water is called bleed water [2, 3, 9–12]. Bleeding becomes negligible either when an equilibrium has been reached among the gravitational, inter-particle and other physicochemical forces, or when hydration, setting or other reactions in concrete start to dominate [2, 10].

Bleed water can accumulate at the top of a cement-based material either by uniform seepage (termed normal bleeding), or through the formation of channels and craters (termed channelled bleeding) [2, 10, 13]. For concrete, bleed water can also be trapped under or around coarse aggregate and reinforcement. In contrast to external bleeding which collects at the top of the material, this phenomenon is known as internal bleeding. The European Federation of Foundation Contractors (EFFC) and the Deep Foundation Institute (DFI) also define bleeding as the upward migration of water in contrast to the sideways seepage due to filtration [1]. Different zones are formed as a result of the particle and water movements. In Powers' experiments on cement pastes [13], four zones are identified:

- A zone of clear water at the top;
- A zone with the original density;
- A zone of increasing density towards the bottom;
- A zone of maximum compaction with uniform density.

However, there was no maximum compaction zone found in Powers' experiments on concrete [2], so only three zones were identified in concrete.

The various zones formed inside cement-based materials are illustrated in Figures 2.1 to 2.3 [2, 12, 13]. Normal bleeding and internal bleeding can be respectively seen in Figures 1.2 and 1.7. Figures 2.4 and 2.5 show the channels and craters observed in the PPC test and the experiment from Massoussi et al. [14].

Bleeding rate and bleeding capacity are two critical parameters in the quantification of bleeding [1–3]. Bleeding rate is the rate at which bleed water is expelled from cement-based materials, while bleeding capacity is the amount of bleed water that accumulates on top of cement-based materials before concrete has set [3]. Other literature [2, 15] also defines bleeding rate as the rate of concrete volume contraction, and bleeding capacity as the total reduction of concrete volume when internal bleeding is assumed to be insignificant. There are two stages identified during bleeding; an initial stage with a constant rate of bleeding, followed by a stage with a reducing bleeding rate, as shown in Figure 2.7 [2, 3, 9–12].

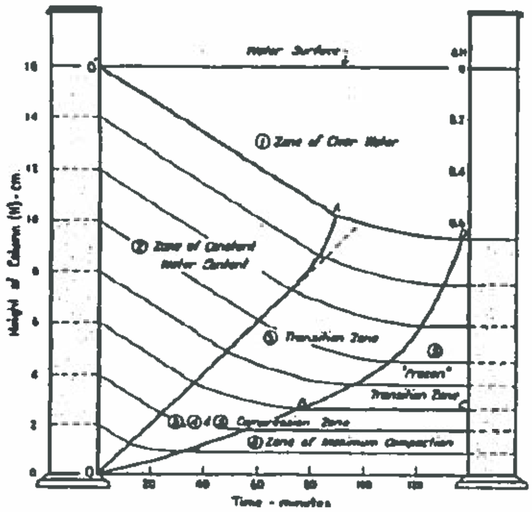

Figure 2.1: Zones in cement paste [2]

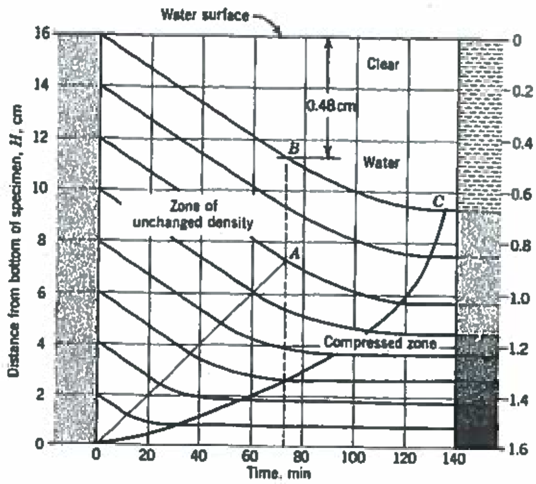

Figure 2.2: Zones in concrete [13]

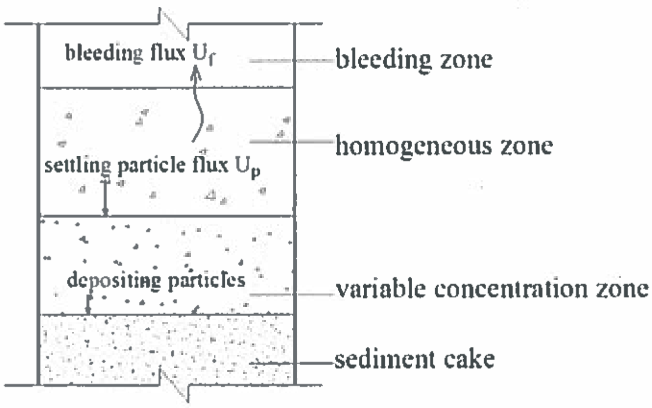

Figure 2.3: Zones in modern cement paste [12]

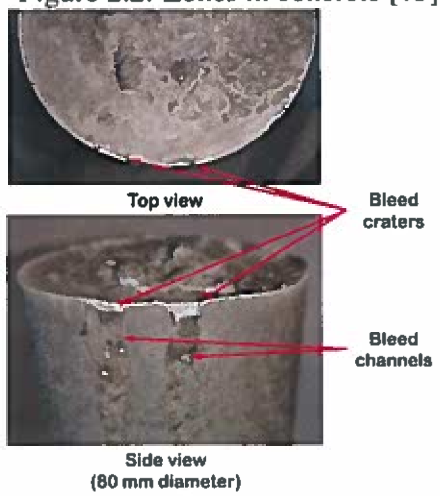

Figure 2.4: Bleed channels and craters (PPC test)

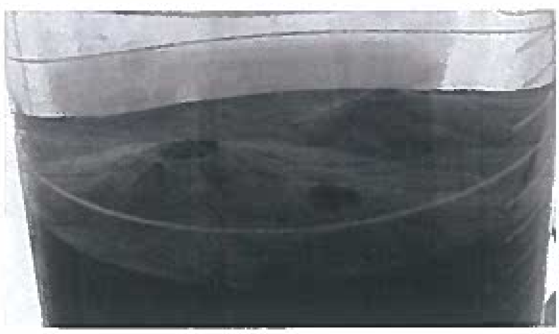

Figure 2.5: Bleed craters (cement paste) [14]

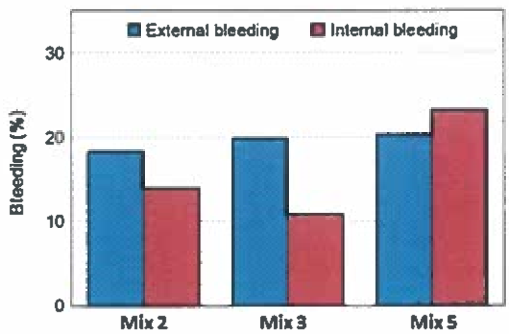

Figure 2.6: External and internal bleeding [15]

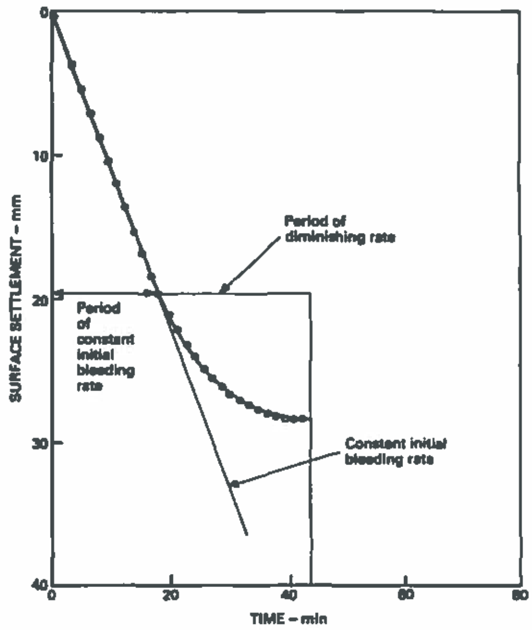

Figure 2.7: Two stages of bleeding [10]

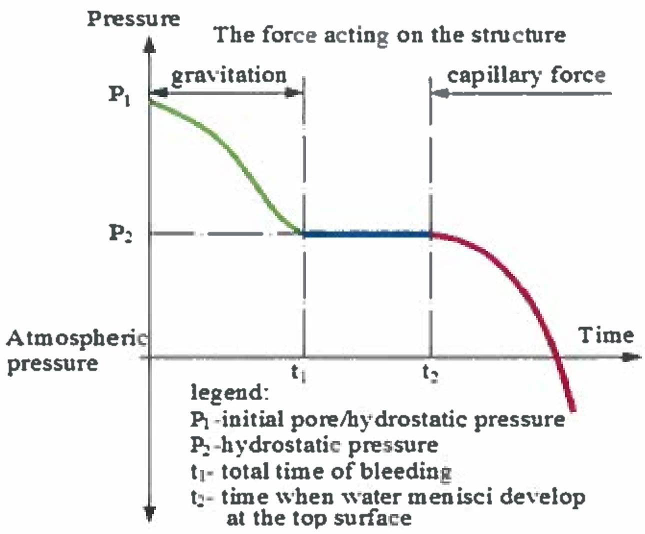

Figure 2.8: Radocea's prediction of pore pressure variation [12, 16]

2.2 Current Models of Bleeding

This section presents current theories that describe bleeding of cement-based materials. There are two main models describing the bleeding processes, sedimentation and consolidation [2, 3, 9–12, 14, 15, 17].

2.2.1 Sedimentation Model

The sedimentation model describes bleeding in terms of identical layers of particles falling through water, and it is based on Poiseuille's law of capillary flow [2, 9, 10, 17]. It is analogous to water flowing through a solid body with a large number of identical, parallel and cylindrical capillaries [2].

During the constant rate period, Powers suggests that Darcy's law using the Kozeny-Carman model for the coefficient of permeability (K) should control the bleeding process in cement-based materials. Equations (2.1) and (2.2) give calculations for a constant bleeding rate in cement paste [2]. The concrete bleeding rate can be correlated with the cement paste results via Equation (2.3) [2].

$$Q = K\frac{\Delta h}{L} \tag{2.1}$$

$$K = \frac{\rho_w g}{k_c \eta x^2}\frac{(\varepsilon - w_i)^3}{(1-\varepsilon)^2} \tag{2.2}$$

$$\frac{Q_{concrete}}{Q_{paste}} = \left(\frac{P}{V}\right)^2 \frac{\rho_{s,avg} - \rho_w}{\rho_c^o - \rho_w} \frac{1+m}{1+m(\frac{x_{ag}}{x_c})} \tag{2.3}$$

Here, Q is the flow rate (m/s) and, hence, the bleeding rate; Δh is the change of the hydraulic head (m) over a depth L (m); K is the coefficient of permeability (m/s); ρ_w is the density of water; g is the gravitational constant (m/s^2) ; k_c is the Carman constant; η is the viscosity (kg/ms); ε is the porosity; x is specific surface area (m^2/m^3); w_i is the empirical constant representing the immobile water; p/V is the dimensionless paste content of concrete; m represents a dimensionless mix based on volume; $\rho_{s,avg}$ is the average solid density in concrete; ρ_c^o is the apparent density of cement in water; x_{ag}/x_c is the specific surface area ratio of aggregate to cement.

Steinour developed bleeding capacity equations for cement paste, presented in Equations (2.4) and (2.5) [13, 17]. Based on experimental results, Powers further provided an inequality (Equation (2.6)) of bleeding capacities between cement paste and concrete [2].

$$\Delta H_{paste} = m_s^2 c[w/c - (w/c)_m]^2 \tag{2.4}$$

$$c = c_B(1 - \Delta H_{paste})^3 \tag{2.5}$$

$$\frac{\Delta H_{concrete}}{p/V} \leq \Delta H_{paste} \tag{2.6}$$

Here, ΔH is the bleeding capacity representing the ratio of total bleed water to the net mixing water; m_s is the slope of the line relating $\sqrt{\Delta H_{paste}}$ and w/c from curve-fit of the experimental data. c is the cement in the mix; c_B is the volume of cement per unit of the base volume; w/c is the water-cement ratio by volume.

Radocea's experiment [9] for pore pressure measurement confirmed Powers' theory about the constant bleeding rate of a thin-layer (about 50 mm) cement paste. Equation (2.7) relating the pore pressure dissipation rate to the bleeding rate was used by Radocea to confirm Powers' theory. Here, ρ_c is the cement paste density (kg/m^3) and u_{ex} is the excess pore pressure (kPa).

$$Q_{paste} = \frac{1 - w_i}{g(\rho_c - \rho_w)(1 - \varepsilon)} \left| \frac{\Delta u_{ex}}{\Delta t} \right| \tag{2.7}$$

Figure 2.8 predicts the pore pressure variation of cement pastes from later research of Radocea [16, 12], but there is not a thorough explanation about how this plot was produced. The convex green part of this plot represents the bleeding phase. This plot from Radocea is confirmed by a recent study on bleeding of modern cement pastes from Peng et al. [12].

2.2.2 Consolidation Model

From experiments studying cement pastes of increasing depths, Tan et al. [10] suggest that the self-weight consolidation model provides a better explanation of the bleeding phenomenon than sedimentation. Tan et al. [10] employed the Terzaghi's one-dimensional consolidation equation to derive expressions for the surface settlement whose time derivative is the bleeding rate (Equations (2.8) and (2.9)) [10]. The horizontal asymptote of the surface subsidence indicates the final bleeding capacity.

The entire derivation uses the cement-water ratio by volume (e). e_0 the initial volume ratio; a is the factored depth of the actual depth z (Equation (2.13)); $s(t)$ is the surface subsidence (bleed height);

C_F and β are derived coefficients and found by fitting the experimental results (Equations (2.11) and (2.12)).

$$s(t) = \frac{\beta}{2}\left(\frac{L_0}{1+e_0}\right)^2 \left\{1-\sum_{n=0}^{\infty}(-1)^n \frac{4}{\lambda_n^3} exp\left[-\lambda_n^2 C_F \left(\frac{1+{e_0}^2}{L_0}\right)t\right]\right\} \tag{2.8}$$

$$\begin{aligned} Q_{paste}(t) &= \frac{ds}{dt} \\ &= 2\beta C_F \sum_{n=0}^{\infty}(-1)^n \frac{1}{\lambda_n^3} exp\left[-\lambda_n^2 C_F \left(\frac{1+{e_0}^2}{L_0}\right)t\right] \end{aligned} \tag{2.9}$$

$$\lambda_n = \frac{2n+1}{2}\pi \tag{2.10}$$

$$C_F \frac{\partial^2 e}{\partial a^2} = \frac{\partial e}{\partial t} \tag{2.11}$$

$$\beta = \frac{\partial e}{\partial a} \tag{2.12}$$

$$da = \frac{dz}{1+e_0} \tag{2.13}$$

Yim et al. [15] developed a more comprehensive model for self-weight consolidation of concrete based on the small-strain theory of linear poroelasticity. The pore pressure $u(z,t)$ and the surface subsidence $s(t)$ are:

$$u(z,t) = \frac{\zeta \eta \gamma_{concrete} z c_d}{M_{concrete} K} erf\left(\frac{z}{\sqrt{4c_d t}}\right) \tag{2.14}$$

$$\begin{aligned} s(t) &= \\ &\frac{\gamma_{concrete} L_0^2}{2M_{concrete}}\left[1-erf\left(\frac{L_0}{\sqrt{4c_d t}}\right)\right] + \frac{\gamma_{concrete} c_d t}{M_{concrete}} erf\left(\frac{L_0}{\sqrt{4c_d t}}\right) - \sqrt{\frac{\gamma_{concrete}^2 L_0^2 c_d t}{\pi M_{concrete}^2}} exp\left(-\frac{L_0^2}{4c_d t}\right) \end{aligned} \tag{2.15}$$

$$M_{concrete} = \frac{M_{mortar}}{1-\phi} \tag{2.16}$$

$$\nabla^2 u = \frac{1}{c_d}\frac{\partial u}{\partial t} \tag{2.17}$$

Here, $\gamma_{concrete}$ is the sample unit weight; ζ is the Biot coefficient; c_d is the diffusivity (defined in Equation 2.17); M is the oedometric modulus; ϕ is the volume fraction of the coarse aggregate. M_{mortar} is evaluated from the experimental measurement. The bleeding rate ($Q(t)$) can be found by the time derivative of surface subsidence ($s(t)$).

2.2.3 Remarks on Two Models

Although there are different solutions and theories proposed for the bleeding phenomenon, the mechanisms behind bleeding are still not clearly demonstrated and agreed by all researchers [1–3, 9–15, 17].

For studies based on cement paste, the sedimentation model deals with the bleeding rate and capacity separately. Tan et al. [2, 13] also showed that an increase in the sample depth could change the underlying mechanism from sedimentation to consolidation. However, Radocea [9] still confirmed a part of the Powers' sedimentation model by the pore pressure measurement, and Tan et al. [10] did not thoroughly check the bleeding capacity based on the consolidation model as their experiments terminated around 30 minutes to minimise the hydration effect. Nevertheless, both models do not clearly explain the diminishing stage.

For research on concrete bleeding, models are normally developed based on cement paste studies [1, 2, 12, 18]. This may underestimate the effect of coarse aggregate as implied by internal bleeding and channel formation [3, 11, 15]. The sedimentation and consolidation models are employed arbitrarily in research without any explanation for not using the other [1, 2, 11, 12, 15, 18]. It may cause confusions in the construction industry to simply combine the results and suggestions from different theories. Furthermore, these concerns may be magnified for modern concrete, such as tremie concrete, which has a higher content of fine particles and contains various chemical admixtures [12]. Although comprehensive theoretical solutions are provided in the study of Yim et al. [15], their novel experiments seem to have taken considerable time and only a small part of their theory was compared to experiments [15, 11]. This is discussed further in the following sections.

2.3 Experiments, Apparatus and Methods

This section outlines the experiments, apparatus and methods employed to study bleeding and other relevant properties of cement-based materials.

2.3.1 Experiments and Apparatus

Most studies on bleeding directly measure bleeding volume or surface subsidence (bleed height) [2, 8, 11, 12, 18–22]. The standard test described by the American Society for Testing Materials (ASTM) and the British Standard Institution (BSI) involves manually collecting and measuring the bleeding water and this is the most common test method used in the construction industry (Figure 2.9) [8, 20]. Powers [2] used the float method to read the surface subsidence of a glass fibre on the disk at the centre of the sample (Figure 2.10). Yim et al. [11, 15] applied non-contact laser displacement sensors to measure the relative displacement between the concrete surface and free water surface (Figure 2.11). Josserand et al. [19, 23] collected bleeding water by making tracks on the top of the sample (Figure 2.12). Lastly, although the apparatus was applied for permeability measurement, Picandet et al. [21] used an oedometer with a displacement transducer (Figure 2.13).
Pore pressure was also measured in most of the experiments [9, 11, 12, 18, 21, 22]. Peng et al. [12, 18] developed the HYdroStatic Pressure Test (HYSPT) in which pressure sensors can be attached at different depths (Figure 2.14). Radocea's experiment [9] used a single pressure transducer measuring pore pressure at a fixed depth (Figure 2.15). Yim et al. [11] equipped a pressure sensor at the bottom of a pressure vessel (Figure 2.16). A pore pressure transducer was also used at the bottom of the controlled oedometer from Picandet et al. [21, 22] (Figure 2.13).

Pressurised apparatus can also be employed to simulate bleeding. As mentioned above, Yim et al. [11] used pressurised vessel (Figure 2.16). The BAUER test with the BAUER filter press (Figure 2.17) is another pressurised test that can be applied in situ [1, 24].

Furthermore, Peng et al. utilised a Turbiscan to measure turbidity and, thus, the bleed water of modern concrete with chemical admixtures [12]. The application of ^1H low-field nuclear magnetic resonance (NMR) provides another novel method of assessing bleeding [25]. It distinguishes the water on the top of the cement paste in the transition layer and in the cement paste by examining the transverse relaxation time (T_2) of ^1H protons.

2.3.2 Methods

From the background research, bleeding can be reduced by up to seven different methods [3]:

1. Reducing water content or water-binder ratio;
2. Increasing the fineness of the cementitious materials;
3. Increasing the amount of fine sand;
4. Using supplementary cementing materials such as fly ash, slag, or silica fume;
5. Using blended hydraulic cements;
6. Using chemical admixtures (e.g. superplasticiser);
7. Using air-entrained concrete.

In this project, three methods (including water content, and amount of fine sand and superplasticiser) were employed to produce extreme cases of bleeding and examined the validity of the PPC test.

After the preliminary tests and site tests, a discrepancy was found between the laboratory test results and the site test results obtained with the same apparatus. It was found that dry aggregate was directly used to prepare laboratory tremie concrete comparing with the saturated aggregate used in construction tremie concrete. Therefore, it suggested that the water absorption of dry aggregate in laboratory tremie concrete might affect the test results [5, 11, 15, 26–28]. Further literature review [5] indicated that saturated and surface-dry aggregate (Figure 2.18) should be used to prepare tremie concrete in order to eliminate the effect of the water absorption on the actual mixing water of tremie concrete. Therefore, an additional step of pre-saturation was added to the experiment and the bleeding behaviours were proved to be similar between the site and laboratory tremie concrete.

As Powers [2] has studied the effect of the specific surface area (= surface area/volume) on bleeding of traditional cementitious materials with a great depth, this project further investigated how the specific surface area affected bleeding of modern tremie concrete. From Powers' studies [2], the bleeding rate of a cementitious material is related to the average falling speed of particles. The speed of a particle is controlled by the difference between the downward self-weight of the particle and the upward viscous drag from water. The viscous drag is proportional to the surface area of the particle and the self-weight is proportional to the volume of the particle, so the greater specific surface area of a particle the slower its falling speed. Since fine sand has a much greater specific surface area than coarse aggregate, increase the amount of fine sand will increase the specific surface area of the mix design when all relevant parameters (including total mass, aggregate and water-binder ratios, etc.) are kept constant. Therefore, the amount of fine sand was examined further in the specific surface area tests of this project. In following chapters, it is also shown that there is less effect on bleeding if only the amount of fine sand is changed regardless of other relevant parameters.

Figure 2.9: Apparatus for site tests [20, 8]

Figure 2.10: Float method [2]

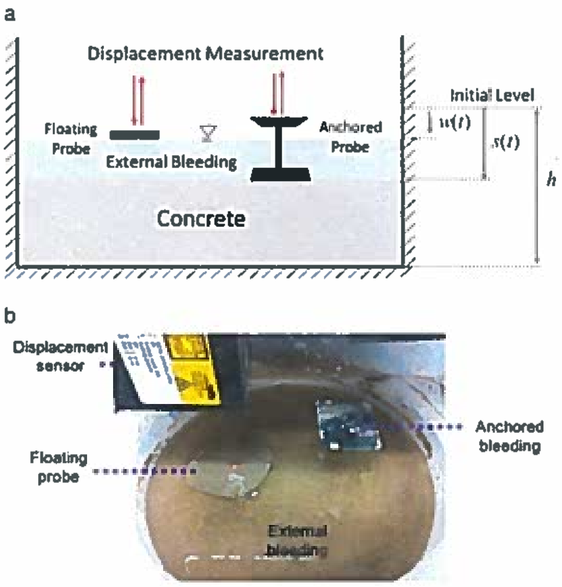

Figure 2.11: Laser displacement sensors [15, 11]

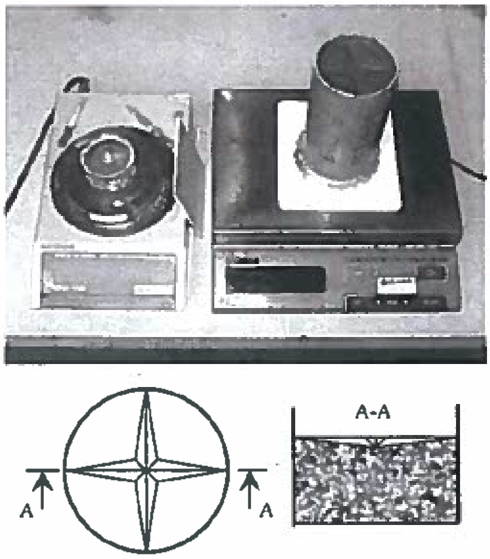

Figure 2.12: Tracks water collection [19, 23]

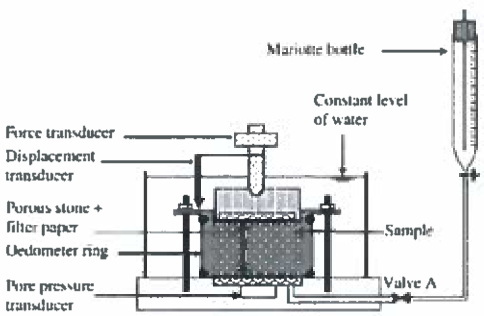

Figure 2.13: Modified Oedometer [21, 22]

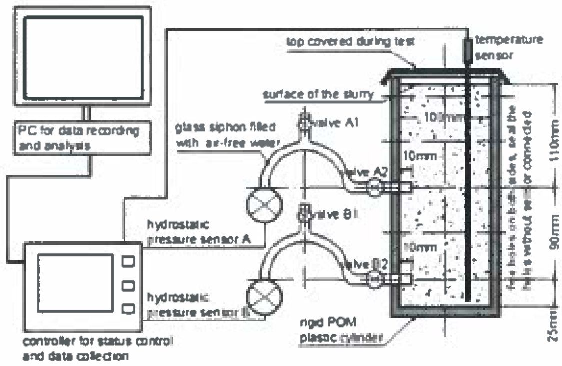

Figure 2.14: HYdroStatic Pressure Test (HYSPT) [12]

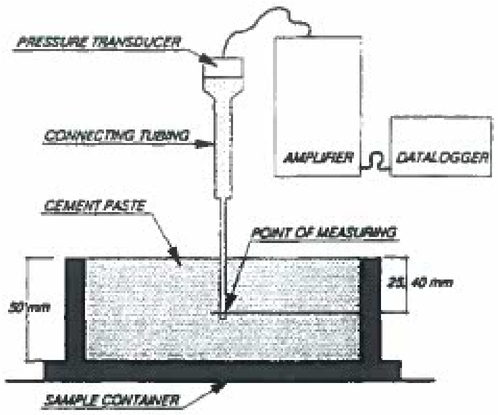

Figure 2.15: Radocea's experiment [9]

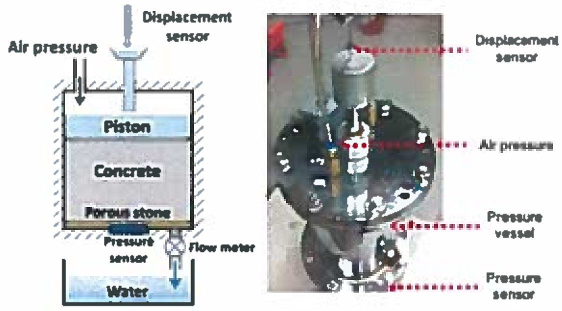

Figure 2.16: Pressure vessel [11]

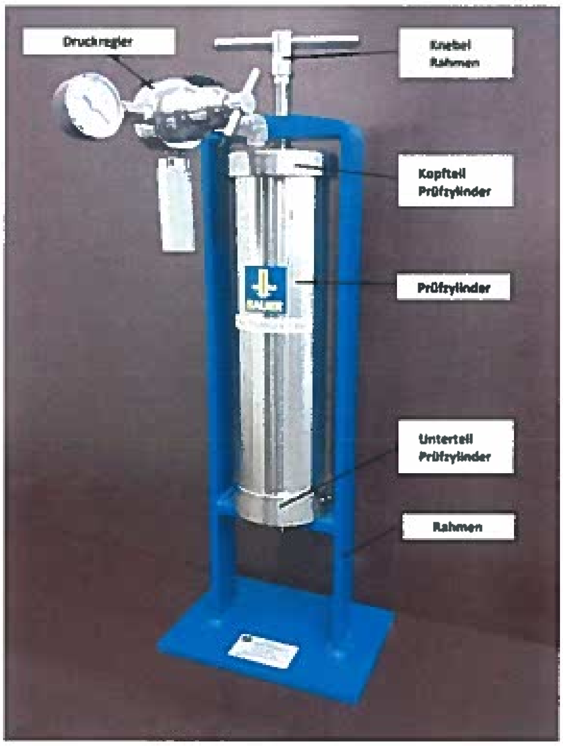

Figure 2.17: BAUER concrete filter press [24]

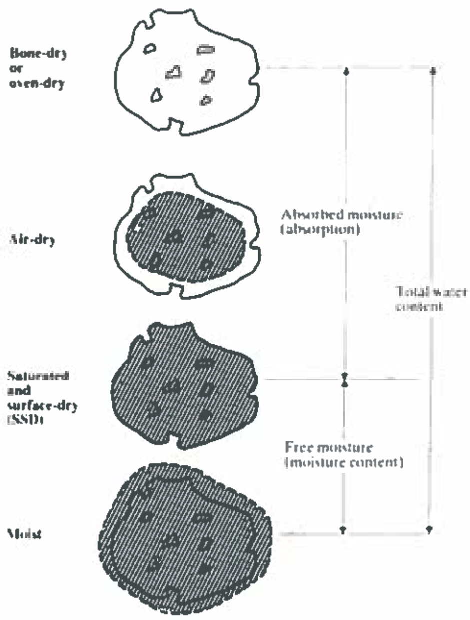

Figure 2.18: Moisture in aggregate [5]

2.4 Opportunity for Further Study

Although there are many studies on the bleeding phenomenon of cement-based materials, some of them start to become outdated due to developments in the cement and concrete technologies. Moreover, there is a clear gap between previous studies and their applications in the construction industry.

In the case of modern concrete such as SCC, the concepts and definitions used to characterise the bleeding process of traditional cementitious materials start to become inaccurate. The observation of bleed water accumulation may not allow the bleeding process to be correctly followed. The top bleed water layer can be less sharp in modern concrete than in traditional concrete due to the high content of fine particles and the application of chemical admixtures (superplasticiser) [12]. Rather than clear bleed water, mortar and grout are expelled during the bleeding of modern concrete, as indicated in the grout volcano (Figures 1.3) [4, 12]. It is also hard to distinguish grout and mortar from modern concrete by visual observation. Even defining bleeding in terms of volume contraction can be uncertain, as voids created due to internal bleeding can reduce volume contraction. The histogram in Figure 2.6 from the study by Yim et al. [15] shows that internal bleeding can be comparable to external bleeding in concrete.

While sedimentation and consolidation models of bleeding have been developed for a long time and various expressions are provided in different studies, there are still inadequate studies confirming those models independently and investigating their suitability under different circumstances. Although the study of modern cement pastes from Peng et al. [12] recently validated Radocea's prediction of the pore pressure variation (Figure 2.8), it is ambiguous as only a single experimental result from that study shows a convex shape and is used to confirm the Radocea's prediction. The other more than 10 pore pressure measurements in the same study from Peng et al. [12] are either close to a straight line or a concave shape, so the confirmation from Peng et al. [12] is not convincing. Moreover, in most solutions, a great number of parameters are required to be measured by different methods before the actual calculations of the bleeding rate and bleeding capacity. This will considerably affect the applicability of those solutions in the construction industry.

For the existing experiments, cement-based materials in many studies are not similar to modern concrete used in construction. Internal bleeding and less sharp bleed water layer in modern concrete cause concerns about the accuracy and practicality of experiments (and even site tests) that directly measure the volume of bleed water or surface subsidence [4, 11, 12, 15]. Furthermore, Yim et al. [11] highlight issues with applying pressurised apparatus to bleeding analysis (Figures 2.16 and 2.17). For example, pressurised air can partially infiltrate or fill voids, leading to a decrease of pressure towards the bottom of the sample. It is also doubtful whether the pressurised apparatus is purely investigating the bleeding alone, since bleeding is upward migration of water but the pressurised apparatus collects water at the bottom [3]. Finally, many novel experiments are only developed for the use in the laboratory and there are hardly any attempts to apply new methods on site.

Therefore, the above-mentioned issues provided a unique opportunity for this project to investigate the bleeding of a specific modern concrete (tremie concrete) under real-world circumstance (construction of deep foundations). Apart from validating one of the bleeding models, this project also focused on creating a link between the bleeding studies and the construction industry (especially for deep foundations). This was achieved by proposing a simplified bleeding model that can be more easily applied in the industry. Then, a corresponding experiment was developed to solely analyse the bleeding effect and to be used on site for this specific type of modern concrete (tremie concrete). The proposed model and developed experiment are presented in following chapters.

3 Proposed One-dimentsional Self-Weight Consolidation Model

In this project, tremie concrete was expected to consolidate one-dimensionally under its self-weight because of the size of the deep foundation, then undergo considerable consolidation because of its high workability [1, 4].

Since the situation of a deep foundation is similar to the studies of Yim et al. [11, 15], a consolidation model should provide a better prediction than the sedimentation model. Moreover, the consolidation of tremie concrete is likely to be one-dimensional in deep foundations, as the presence of a filter cake forming from the supporting fluids limits sideways seepage from the foundation to the surrounding soil [1, 5]. The analysis then should be similar to that reported by Tan et al. [10], but the solution focused on the excess pore pressure dissipation.

The proposed mechanism was validated via the pore pressure measurement which is the driver of the consolidation mechanism. A pore pressure measurement can avoid problems caused by internal bleeding or turbid water layers; factors that can lead to inaccuracy in surface subsidence measurements. Moreover, the pore pressure measurement can also confirm the consolidation model in general. The pore pressure was consequently expected to support the self-weight of tremie concrete immediately after the mixing, and decrease back to the static condition after the completion of the consolidation process [29, 30].

Furthermore, there is a clear correlation between the pore pressure measurement and the bleeding measurement. Equations (2.7) (given in the previous chapter) and (3.1) (provided below) from previous studies [9, 12, 18] show that the surface subsidence (s) is directly proportional to the pore pressure (u), and the bleeding rate ($Q = ds/dt$) is directly proportional to the pore pressure dissipation rate ($\partial u/\partial t$). Since the pore pressure measurement (given in the following chapters) can be more accurate and less susceptible to human error than the manual bleeding volume measurement on site, the pore pressure measurement can be a better way of analysing bleeding on site in the future.

$$u(L,t) = \rho_w g s(t) + [\rho_s \Phi_0 + \rho_w (1 - \Phi_0)] g (L - s(t)) \tag{3.1}$$

Here, ρ_w and ρ_s are the water and solid densities. Φ_0 is the initial solid fraction at depth L.

In following sections, Terzaghi's one-dimensional consolidation theory is first introduced. Then, the solutions to the one-dimensional self-weight consolidation model are provided. The apparatus designed for the pore pressure measurement and the validity of the proposed model are explained and discussed in following chapters.

3.1 Terzaghi's One-Dimensional Consolidation Theory

The assumptions for Terzaghi's one-dimensional consolidation theory are [10, 29]:

- Tremie concrete is homogeneous;
- Particles and water are incompressible (all volumes remain unchanged);

- Small-strain assumption: coefficient of permeability (K) and small element stiffness (E'_0) are constant.

Terzaghi's equation for a small unit area ($A = 1\ m^2$) element (Figure 3.1) can be derived by [29, 30]:

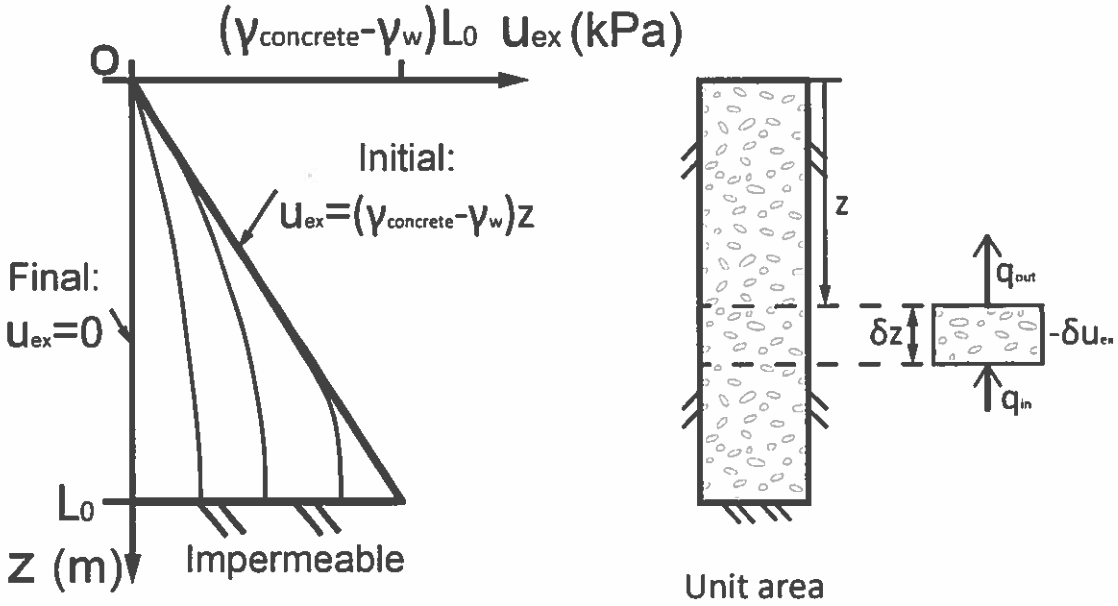

Figure 3.1: Excess pore pressure variation for consolidation under self-weight

$Volume\ reduction = water\ outflow$

$$\delta s A = (q_{out} - q_{in})\delta t \tag{3.2}$$

$$\delta s = \delta q \delta t \tag{3.3}$$

Here, q is the flow rate (m^3/s). Settlement (δs (m)) is calculated from the change in stress (σ'_v (kPa)):

$$\delta s = \frac{\delta \sigma'_v}{E'_0}\delta z \tag{3.4}$$

$$Equilibrium: \ \delta \sigma'_v = -\delta u_{ex} \tag{3.5}$$

$$\delta s = -\frac{\delta u_{ex}}{E'_0}\delta z \tag{3.6}$$

From Darcy's law with hydraulic gradient (i):

$$Darcy's\ law: \ \delta q = -KiA \tag{3.7}$$

$$\delta q = -\frac{K}{\gamma_w}\frac{\delta u_{ex}}{\delta z} \tag{3.8}$$

Substituting Equations (3.6) and (3.8) into Equation (3.3) with the coefficient of consolidation (C_v (m^2/s)):

$$-\frac{\delta u_{ex}}{E'_0}\delta z = -\frac{K}{\gamma_w}\frac{\delta u_{ex}}{\delta z}\delta t \tag{3.9}$$

$$Terzaghi's\ equation: \ \frac{\partial u_{ex}}{\partial t} = C_v\frac{\partial^2 u_{ex}}{\partial z^2} \tag{3.10}$$

$$C_v = \frac{KE'_0}{\gamma_w} \tag{3.11}$$

3.2 Solutions for Self-Weight Consolidation

The general solution of Terzaghi's equation (Equation (3.10)) expressed in terms of a separable function of two variables time (t (s)) and depth (z (m)) is [30]:

$$u_{ex}(z,t) = [Asin(\lambda z) + Bcos(\lambda z)]exp(-C_v^2 t) + Cz + D \tag{3.12}$$

Here, A, B, C, D and λ are constants. Figure 3.1 schematically shows the process, initial and boundary conditions of consolidation under self-weight with a depth of L_0 [30]:

$$u_{ex}(z=0,t) = 0 \tag{3.13}$$

$$\left.\frac{\partial u_{ex}}{\partial z}\right|_{z=L_0} = 0 \tag{3.14}$$

$$u_{ex}(z,t=0) = (\gamma_{concrete} - \gamma_w)z \ (0 \le z \le L_0) \tag{3.15}$$

$$Symmetry\ requirement:\ u_{ex}(z,t=0) = (\gamma_{concrete} - \gamma_w)(2L_0 - z) \ (L_0 \le z \le 2L_0) \tag{3.16}$$

The solution for the excess pore pressure dissipation (u_{ex} (kPa)) of the self-weight consolidation is:

$$u_{ex}(z,t) = \frac{8(\gamma_{concrete} - \gamma_w)L_0}{\pi^2} \sum_{n=1}^{\infty} \left[\frac{1}{n^2} sin\left(\frac{n\pi}{2}\right) sin\left(\frac{n\pi z}{2L_0}\right) exp\left(-\frac{n^2\pi^2 T}{4}\right)\right] \tag{3.17}$$

The surface subsidence (s (m)) and bleeding rate (Q (m/s)) are given by:

$$\begin{aligned} s(t) &= \frac{1}{E_0'} \int_0^{L_0} [(\gamma_{concrete} - \gamma_w)z - u_{ex}(z,t)]dz \\ &= \frac{(\gamma_{concrete} - \gamma_w)L_0^2}{2E_0'} \left\{1 - \sum_{n=1}^{\infty} \left\{\frac{32}{n^3\pi^3} sin\left(\frac{n\pi}{2}\right)\left[1 - cos\left(\frac{n\pi}{2}\right)\right] exp\left(-\frac{n^2\pi^2 T}{4}\right)\right\}\right\} \end{aligned} \tag{3.18}$$

$$\begin{aligned} Q(t) &= \frac{ds}{dt} \\ &= -\frac{1}{E_0'} \int_0^{L_0} \frac{\partial u_{ex}(z,t)}{\partial t} dz \\ &= \frac{4(\gamma_{concrete} - \gamma_w)K}{\pi \gamma_w} \sum_{n=1}^{\infty} \left\{\left(\frac{1}{n}\right) sin\left(\frac{n\pi}{2}\right)\left[1 - cos\left(\frac{n\pi}{2}\right)\right] exp\left(-\frac{n^2\pi^2 T}{4}\right)\right\} \end{aligned} \tag{3.19}$$

Figure 3.2 shows an example ($C_v = 100 \times 10^{-6}\ m^2/s$) of variations in the excess pore pressure, surface subsidence and bleeding rate (Equations (3.17) to (3.19)) within a unity range and for 6000 seconds (100 minutes); both C_v and time period were similar to experimental conditions in this project, as shown in following chapters. The constant bleeding rate and diminishing rate stages in the bleeding rate plot agree with previous studies [2, 3, 9–12].

Equations (3.18) and (3.19) can provide reliable predictions of bleeding rate and bleeding capacity for the site test with different types of tremie concrete, if the pore pressure variation from Equation (3.17) agrees with experimental data. It is also noteworthy that only a single parameter (C_v) is involved in the excess pore pressure (u_{ex}) calculation, and no more than two parameters in the other two expressions (C_v and E_0' in surface subsidence; C_v and K in bleeding rate). Therefore, these expressions can be more practically applied on site and can help to improve the current industry standard which only has a single average bleeding rate of 0.1 ml/min over a two-hour period [1].

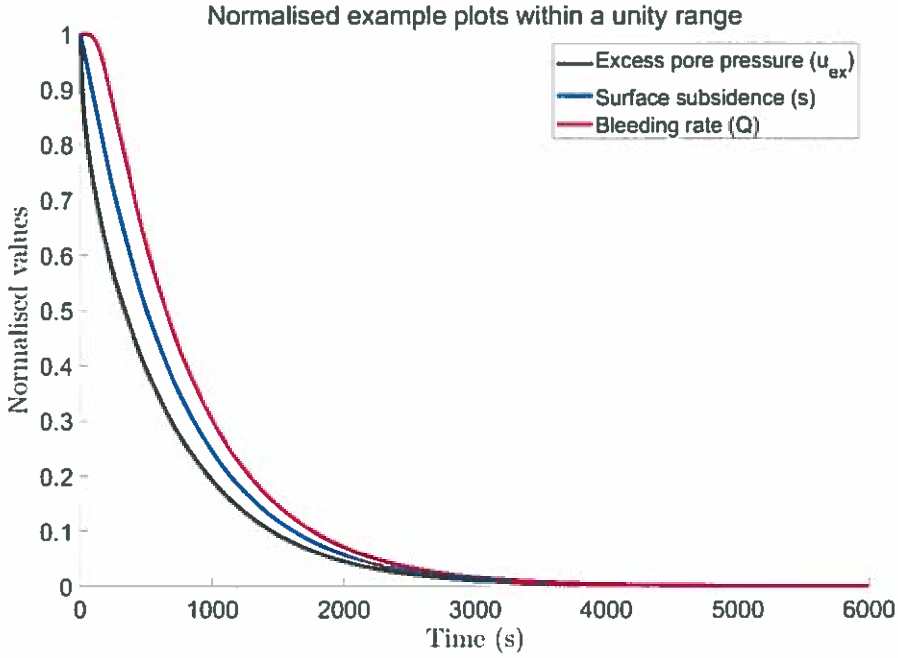

Figure 3.2: Example of the proposed consolidation model

3.3 Comparison with Solutions from Existing Consolidation Models

Comparing with the consolidation models (Equations (2.8) and (2.15)) from Tan et al. [10] and Yim et al. [15] as given in Chapter 2, there is no fundamental difference between the newly developed model in this project and those two existing models as all solutions are based on the consolidation theory. The governing equations of those two consolidation models (Equations (2.11) and (2.17)) are also similar to Terzaghi's equation (which has second derivative in depth and first derivative in time) used in this project.

Nonetheless, solutions of the governing equation in the study from Yim et al. [15] were derived based on the diffusion equation, so error functions are involved in Equations (2.14) and (2.15) of the pore pressure variation and surface subsidence, respectively. There is a little difference between solutions from this project and in the study of Tan et al. [10] (which were derived from the eigenfunction expansion method). However, as mentioned before, this project focused on the comparison between the experimental and theoretical pore pressure variations, and Tan et al. [10] did not derive the solution for the pore pressure variation.

4 Method and Apparatus Development

4.1 Pore Pressure Cylinder (PPC) Apparatus

The layout of the apparatus for the PPC test is shown in Figures 4.1 and 4.2. A 2-litre cylinder with a base diameter of 80 mm was fitted with a tube connection at the bottom (Figure 4.3). A special funnel was added to the top of the cylinder to reduce spillage during the placement and, hence, reduce placing time (Figure 4.4). A filter paper was also placed at the bottom of the cylinder to prevent contamination of the pressure transducer with tremie concrete. A wooden support provided additional stability to the cylinder and prevented it from toppling during the placement of tremie concrete. The cylinder was transparent and fitted with a scale in millimetres, so the bleeding process was observed and the surface subsidence was directly measured during each experiment (Figure 1.2).

The 2-litre cylinder was connected to the pressure transducer via a standard transparent 6 mm tube which was filled with water prior to the placement of tremie concrete. The transparent tube also helped to observe any contamination from tremie concrete. If there was any likelihood of contamination, the valve fitted to the pressure transducer could be closed to reduce potential damage to the pressure transducer. The pore pressure transducer (RS pro 828-5726) measured from 0 kPa to 25 kPa over a voltage range from 0.501 V to 4.500 V, so the calibration factor was 6.25 kPa/V. It was a very sensitive device with high resolution (up to 0.001 mV). A piece of foam was also used to reduce the background noise from the surroundings, and to take up the height difference to the bottom of the cylinder. The data acquisition system (DAQ) converted the analogue input into digital data, before inputting the data into a Raspberry Pi system. In contrast with a desktop computer, the Raspberry Pi device was more portable and, thus, suitable for the site test.

4.2 Concrete Mix Design

A reference mix design from previous studies [31, 32] was used in the experiment A1, as shown in Table 4.1. In the A1 reference mix design, the water-binder ratio was 0.55, the aggregate-binder ratio was 3.6 and the superplasticiser-binder ratio was 0.2%. Apart from the reference mix design in experiment A1, only changes (in mass) from the reference mix design are shown in the corresponding columns in Table 4.1. The aggregate grading curves for different quantities of fine sand amount are shown in Figure 4.5. In the following chapter, it is shown that this mix design with a maximum 10 mm aggregate can produce a similar behaviour, in terms of bleeding, to the actual tremie concrete used in construction.

In the preliminary tests, the water-binder ratio, the amount of fine sand by weight, and the amount of superplasticiser by weight were used to change the bleeding severity in order to examine the validity of the PPC test. Only the amount of one constituent of tremie concrete was changed in each experiment and extreme values were chosen to increase the variability. The water-binder ratios were chosen to be 0.35 and 0.9 for experiments B0 and B1 from the previous study [33]. The amount of fine sand by weight in the aggregate was increased and decreased by 10% for experiments C0 and C1 [28]. The superplasticiser-binder ratio by weight was doubled for experiment A0.

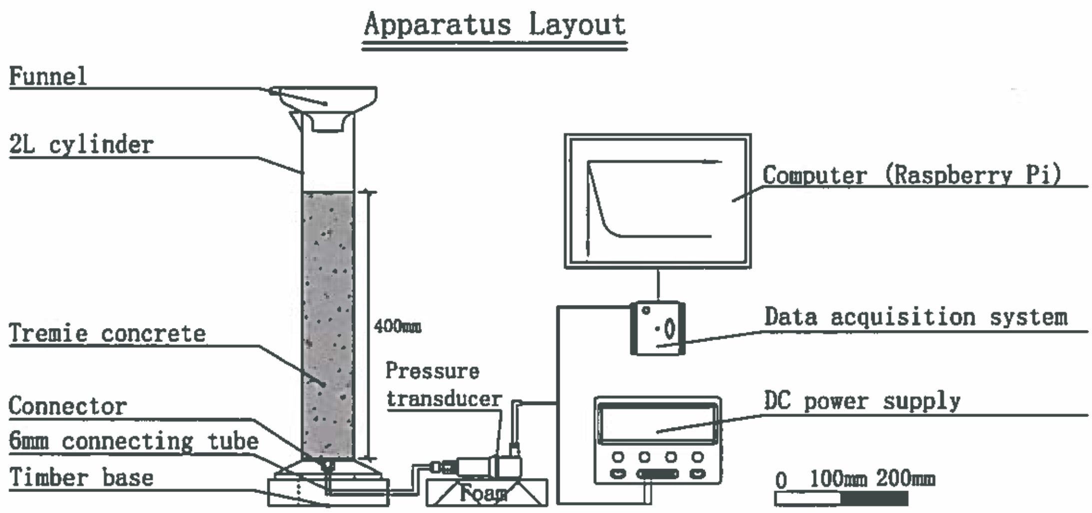

Figure 4.1: Schematic of the PPC apparatus

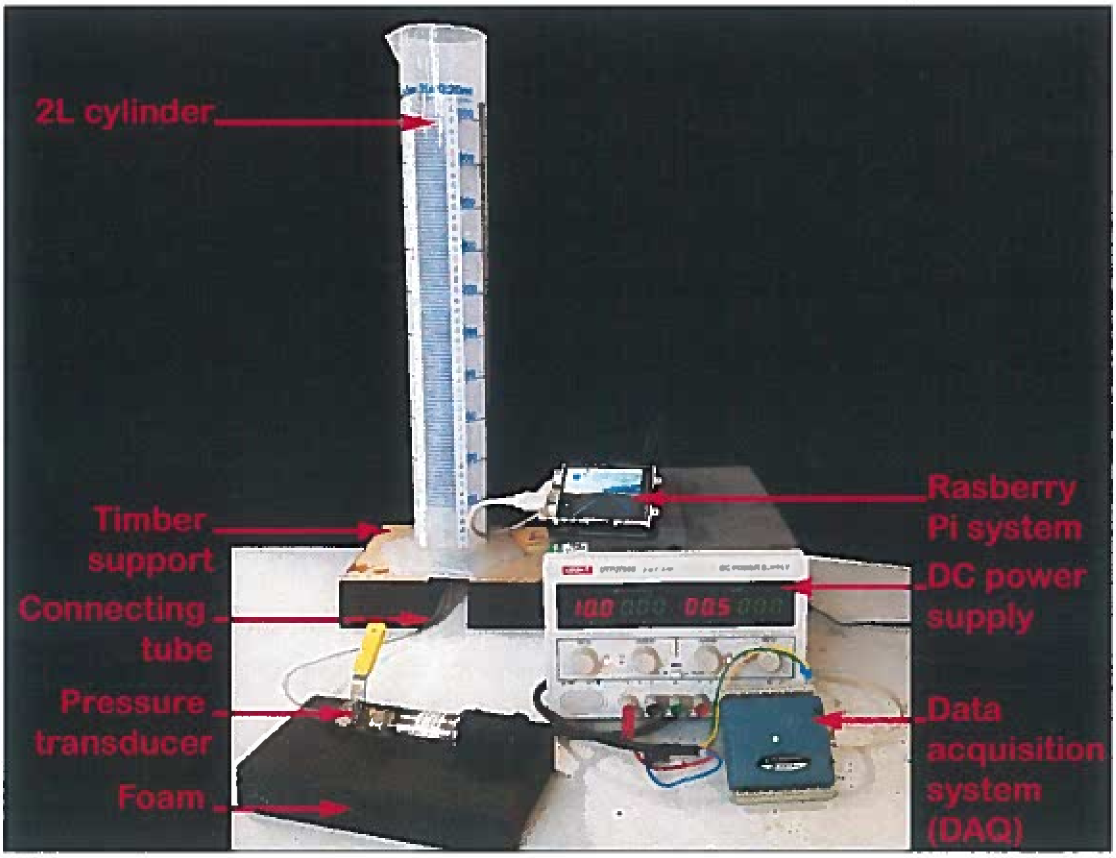

Figure 4.2: Layout of the PPC apparatus

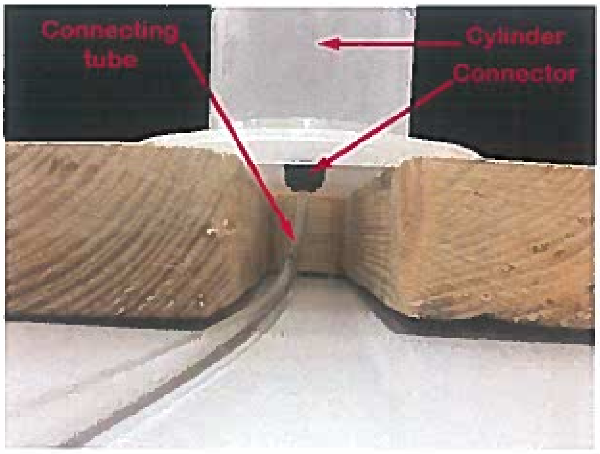

Figure 4.3: Bottom tube connector

Figure 4.4: Special funnel

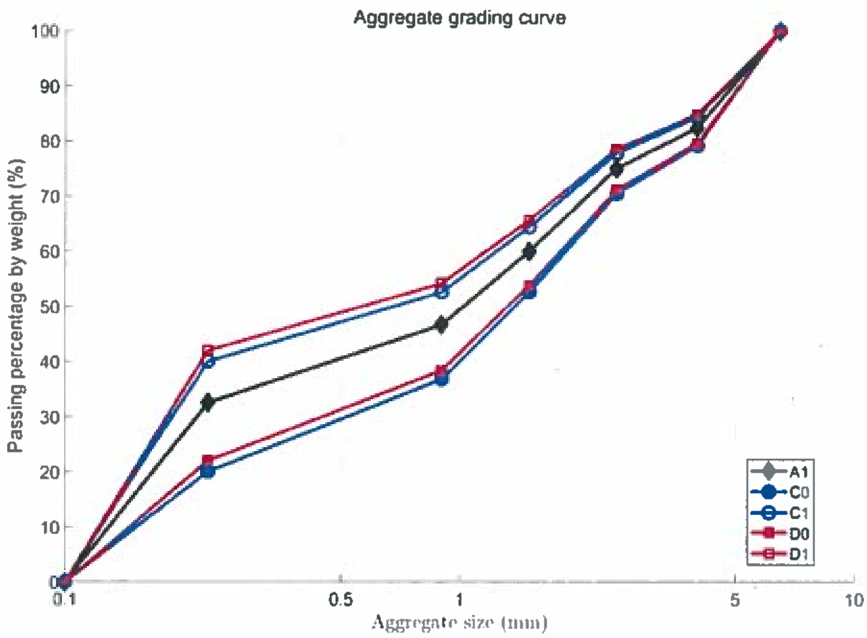

Figure 4.5: Grading curves for different mix design

In the later experiments designed to investigate the effect of changing the specific surface area, it was found that bleeding might not be changed as expected when only the amount of a single constituent was varied [12]. As a result, the C0 and C1 mix designs were adapted to D0 and D1 mix designs by changing the amount of fine sand while maintaining the aggregate-binder ratio and the total mass of the mixture. This is explained in following chapters. A2 was a cement paste, only containing binder materials and superplasticiser. A3 was the same cement paste as A2 with the addition of sand. For both experiments, the total mass and the water-cement and superplasticiser-cement ratios were kept the same.

Mix design			Reference mix design	Super-plasticiser	Water-binder ratio		Fine sand		Specific surface area		Revised fine sand	
			A1	A0	B0	B1	C0	C1	A2	A3	D0	D1
Materials	Producer	Product/Grade	Mass (g)									
Cement and Fly Ash	CEMEX	CEM II/B-V	966						3226	1341		
Fine Sand	Specialist Aggregates	0.15-0.30 mm: 3402	1140				593	1580	0	1582	772	1474
Medium Coarse Sand	Specialist Aggregates	0.40-1.40 mm: 3407	498						0	691.2	575	428
Coarse Sand	Specialist Aggregates	1.00-2.00 mm: 3409	468						0	649.6	541	402
Fine Gravels	Specialist Aggregates	2.00-3.00 mm: 2639F	528						0	0	610	454
Fine Gravels	Specialist Aggregates	3.00-5.00 mm: 2640	258						0	0	298	222
Fine Medium Gravels	Specialist Aggregates	5.00-8.00 mm: 2641	618						0	0	714	531
Total aggregate mass (g)			3510				2963	3950	0	2923	3510	3510
Aggregate-binder ratio			3.6				3.1	4.1	0	2.2	3.6	3.6
Superplasticiser	BASF	SKY 920	2	4					6.5	3		
Superplasticiser-binder ratio			0.2%	0.4%					0.2%	0.2%		
Water			528		870	340			1774	737		
Water-binder ratio			0.55		0.90	0.35			0.55	0.55		
Total tremie concrete mass (g)			5006	5008	5348	4818	4459	5446	5007	5004	5006	5006

Table 4.1: Tremie concrete mix design

4.3 Experimental Procedure

During the preparation period, the 2-litre cylinder was first cleaned and dried. A thin layer of water less than 5 mm was added to the bottom of the cylinder with a trimmed circular filter paper. The pressure transducer and connecting tube were filled with water before connecting to the cylinder. The pressure transducer was filled by a pipette. Air bubbles were expelled by gently tapping the connecting tube.

Before the beginning of each experiment, the initial voltage for zero pore pressure was first recorded without any tremie concrete in the cylinder as there was still a height difference between the bottom of the cylinder and the pore pressure transducer. This initial reading was then subtracted from the experimental data to compensate for the effect of the height difference. The initial mass of water was also measured for each experiment to improve accuracy.

The preparation of tremie concrete involved three steps after weighing out the constituents. The aggregate was first manually mixed for two minutes to produce a uniform mixture of sand and gravel, as well as the addition of 50% of the net mixing water. This mixture was then sealed for 30 minutes to pre-saturate the aggregate. Finally, the binder was added to the mixture and mixed with a handheld stirring mixer for two minutes. The superplasticiser was mixed with the other half of the mixing water and the water-superplasticiser mixture was added to the mixture in three equal measures in the first minute of mixing. There was a negligible time delay from completion of mixing to placement of fresh tremie concrete. The pre-saturation step was omitted in the preliminary tests.

During the test, apart from the bottom pore pressure, the surface subsidence was also manually measured by reading off the scale. The 10- and 30-minute reading intervals from the ASTM and British Standards were changed to 2 minutes in the first 10 minutes, 5 minutes in the following 30 minutes and 30 minutes until 130 minutes, in order to show a clear transition between the two bleeding stages [8, 20].

After the pore pressure had been recorded for two hours, the raw data were analysed, and the experimental samples were left to cure overnight. Samples were extracted for inspection using compressed air. MATLAB codes were developed for theoretical and experimental analysis.

5 Results and Discussion

5.1 Preliminary Tests

All preliminary tests were performed during the Michaelmas term and the pre-saturation stage was omitted. In other words, all the aggregate was oven-dry or air-dry (Figure 2.18). Nonetheless, the aim of the preliminary tests was primarily to validate the practicality of the PPC test, such as health and safety aspects, calibration of the apparatus, repeatability of experimental procedures, reliability of results for different mixes of tremie concrete and possible future on-site application.

The surface subsidence (bleed height) and bottom pore pressure recorded in preliminary tests are shown in Figures 5.1 and 5.2. The bottom pore pressure data were normalised to vary over a unit range in order to remove the inconsistent placement time and multiple peaks from the placement (Figure 5.3). The surface subsidence data were normalised in the same way to compare variations between the bleed height and pore pressure (Figure 5.4). All cured samples are shown in Figures 5.5 to 5.14. The scale next to each sample corresponds to 300 mm.

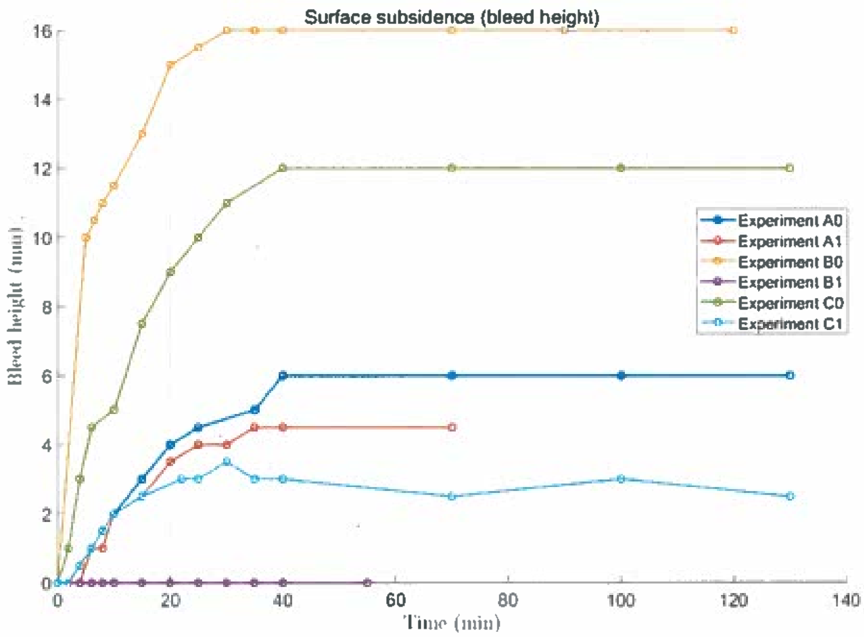

Figure 5.1: Surface subsidence (bleed height) recorded of preliminary tests

From the results (Figures 5.1 to 5.3), the PPC test was determined to be acceptable for the examination of the proposed model. The pore pressure variations were significant and distinguishable in each experiment. The two-hour time scale was also a suitable period for experiments. It also demonstrated the potential to reduce the experimental period to below 20 minutes for the future site application, if only the initial bleeding rate is of interest. In contrast with the surface subsidence plot (Figures 5.1 and 5.4), results from the PPC test (Figures 5.2 and 5.3) are smoother and less susceptible to human error. The order of increase in bleeding rate in Figure 5.4 also approximately aligns with that in Figure 5.3, but the difference is much clearer in the data of the PPC test (Figure 5.3). It was difficult to confidently classify the constant and diminishing rate regions from the manual readings of surface subsidence (Figures 5.1 and 5.4), even though the time periods for readings were refined from the site standards as mentioned in Chapter 4.

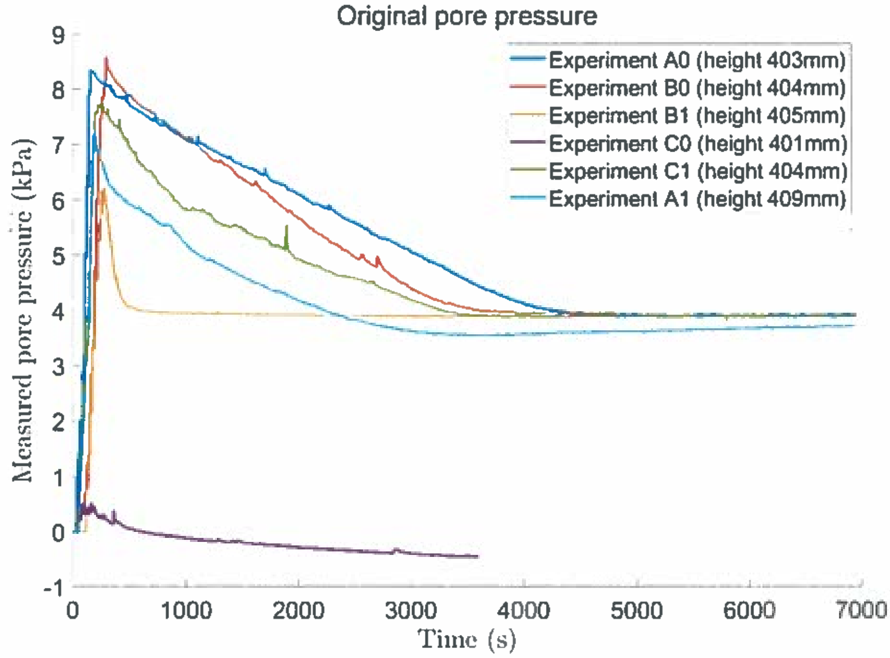

Figure 5.2: Original bottom pore pressure variations recorded of preliminary tests

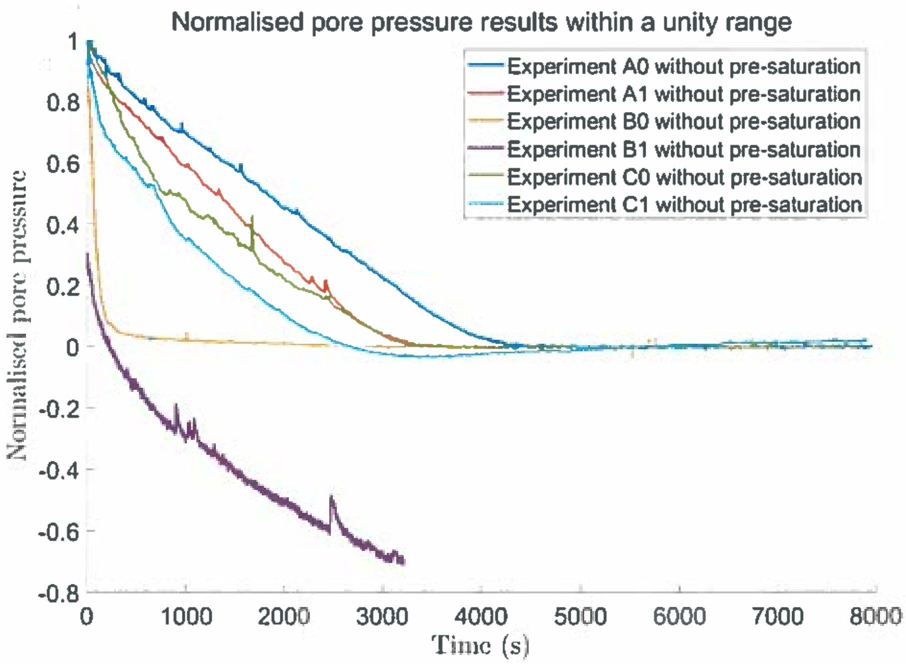

Figure 5.3: Normalised bottom pore pressure variations recorded in preliminary tests

The severity of bleeding in different mixes of tremie concrete was identified by combining observations of cured samples and experimental data. The A0 sample with twice as much superplasticiser as the reference A1 sample had a similar appearance to the reference A1 sample (Figures 5.5 to 5.8), but there was an increase in total bleed water and a decrease in pore pressure dissipation rate

(Figures 5.1 to 5.3). In the high water-binder ratio experiment B0 and low fines experiment C0, many thick channels with craters were seen (Figures 5.10 and 5.12). There was also a significant amount of sand near the top of the B0 specimen, which was probably transported along bleed channels. Experiments B1 and C1 showed little bleeding (Figure 5.1), but insufficient compaction (Figures 5.13 and 5.14). In Figure 5.3, the experiment B1 actually exhibited a situation of negative absorption and it occurred with a decreasing gradient immediately after placement. This might be caused by the absorption, hydration, setting or other reactions taken place in the B1 mix. Nevertheless, in contrast to B0 and B1 experiments, results of C0 and C1 experiments were close to that of the reference A1 experiment, and this is discussed further in Section 5.4.

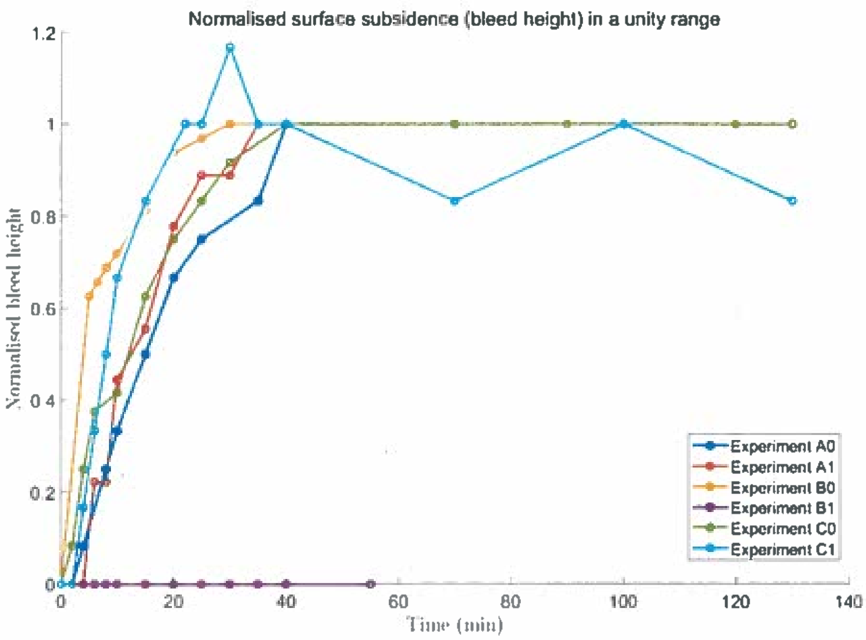

Figure 5.4: Surface subsidence (bleed height) of preliminary tests

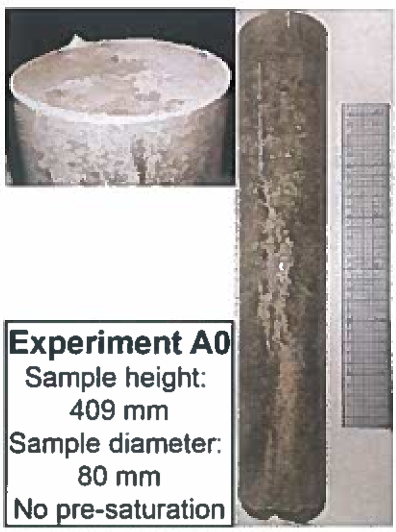

Figure 5.5: Experiment A0

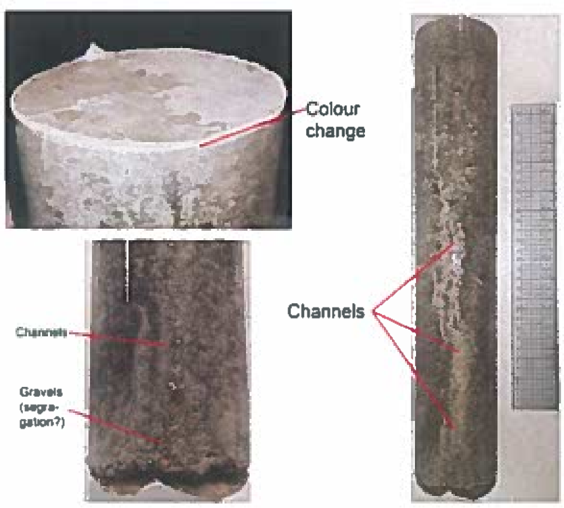

Figure 5.6: Experiment A0 observations

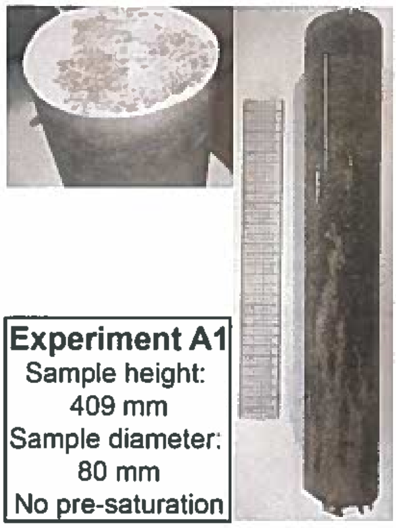

Figure 5.7: Experiment A1

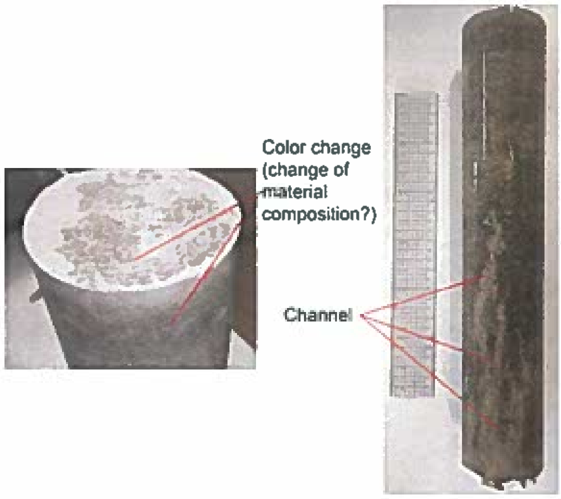

Figure 5.8: Experiment A1 observations

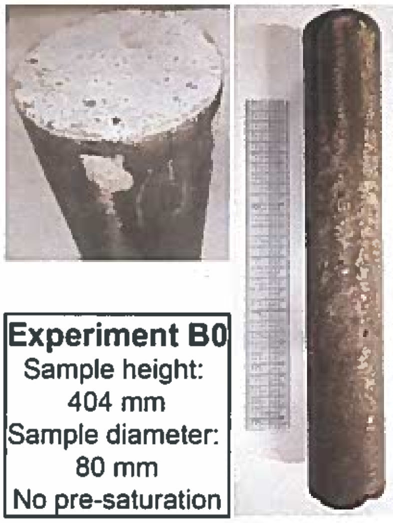

Figure 5.9: Experiment B0

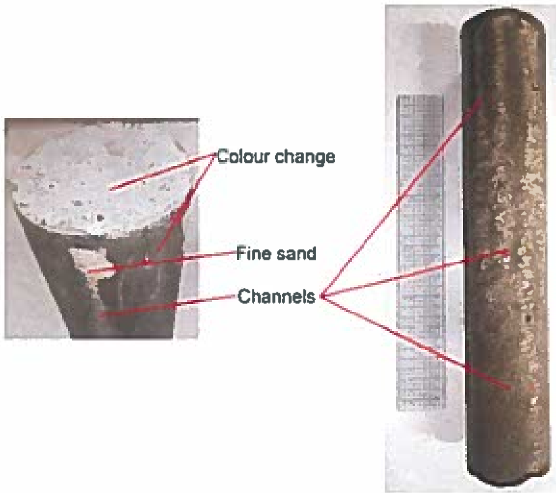

Figure 5.10: Experiment B0 observations

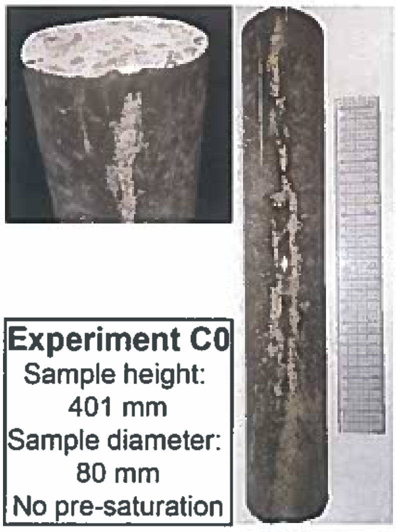

Figure 5.11: Experiment C0

Figure 5.12: Experiment C0 observations

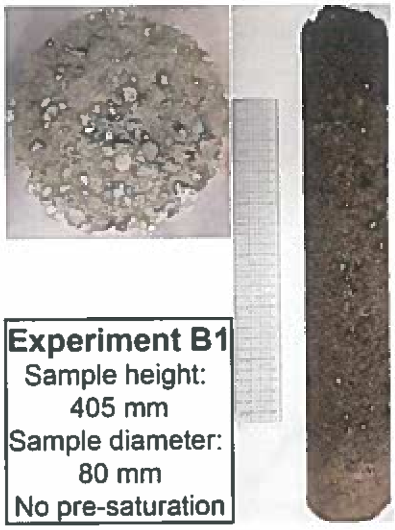

Figure 5.13: Experiment B1

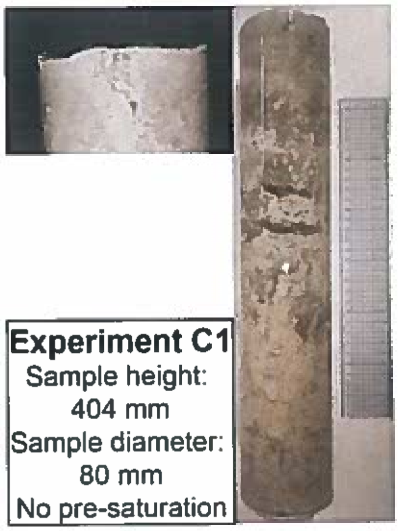

Figure 5.14: Experiment C1

5.2 Site Tests and Pre-Saturation

The PPC test was also performed on-site with real construction tremie concrete, in order to investigate the feasibility of applying the PPC test on-site and to compare the behaviour of the A1 reference mix design with real tremie concrete. The results are shown in Figures 5.15 and 5.16.

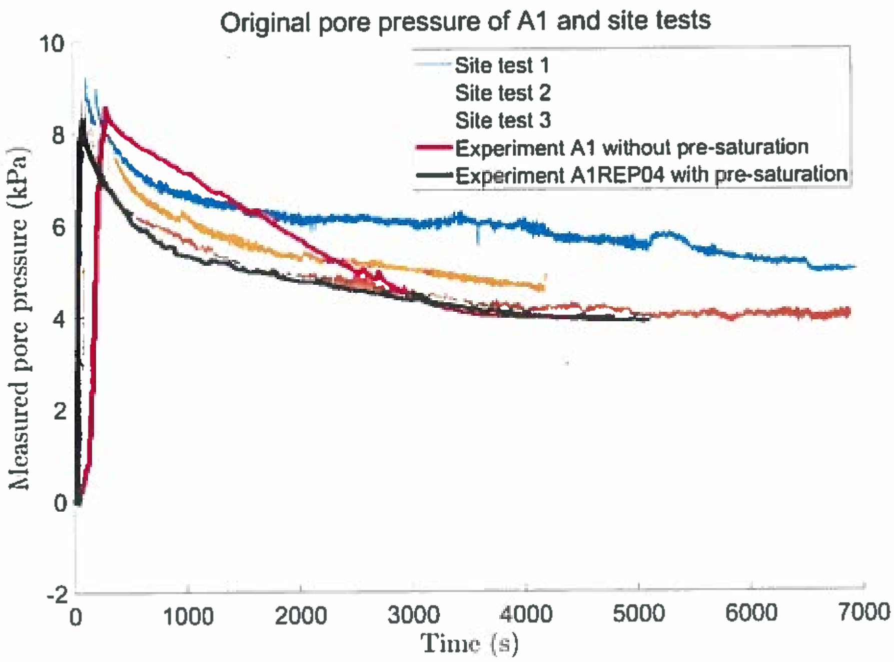

Figure 5.15: Original bottom pore pressure variations of site tests and A1

Although the background noise from the surroundings was more noticeable, recognisable curves (in a shape close to expectation) were still produced from the three on-site tests. The three tests (with similar mix designs) were relatively close but indicated a difference with the preliminary A1 reference test performed in the laboratory.

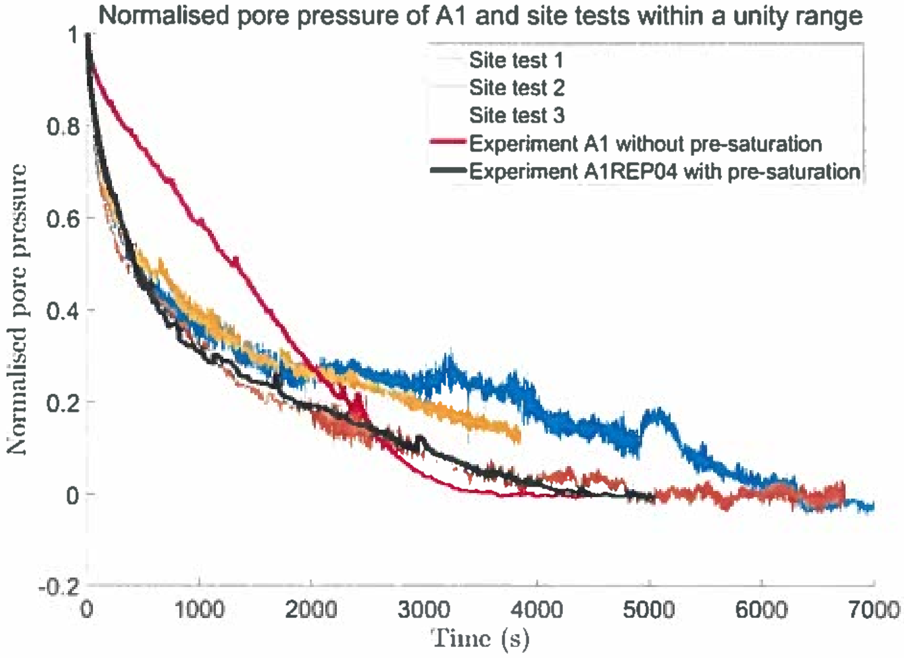

Figure 5.16: Normalised bottom pore pressure variations of site tests and A1

From literature review and suggestions from the site, it was believed that there was a missing pre-saturation step between the laboratory and industrial procedure [5, 11, 15, 26–28]. Without pre-saturation, water would penetrate the pores inside and on the surface of the oven-dry or air-dry aggregate which was used in the laboratory mixture. Water absorption decreased the net mixing water for the A1 reference mix and affected bleeding [5, 15, 11]. The pre-saturation stage was included in all experiments after site tests, so the laboratory tremie concrete closely matched the real-world applications (in terms of bleeding).

The A1 reference mix was then repeated five times (A1REP01 to A1REP05) with a pre-saturation stage and to produce a range of results showing the variation in the A1 reference mix, in a bid to improve accuracy and eliminate any anomalies. Figures 5.17 to 5.20 show the six results obtained from the A1 reference mix design with and without a pre-saturation stage. The manual readings were like those obtained in the preliminary tests, and it was not easy to identify the bleeding stages identified in previous studies [2, 3, 9–12]. On the contrary, three regions (constant rate, diminishing rate and plateau) were recognised in the excess pore pressure dissipation plots (Figure 5.20). Since the bleeding rate is proportional to the pore pressure dissipation rate (Equations (2.7), (3.1) and (3.19)), this led to the confirmation of the mentioned two stages of concrete bleeding in Chapter 2. Despite the spread in results from A1REP01 to A1REP05, there was a clear difference between pre-saturated and non-pre-saturated tremie concrete. This observation was not found in the normalised surface subsidence data (Figures 5.17 and 5.18). This was probably caused by the large inaccuracy from human error in the maximum 6 mm readings (at least $0.5/6 \times 100\% = 8\%$).

Nonetheless, the surface subsidence plots were generally closer to each other than plots in Figure 5.4. Samples of A1REP01 to A1REP05 did not show significant difference (Figures 5.21 to 5.25). Moreover, bleed channels were formed all the way from the bottom to the top of these five repeated samples but not in the A1 sample without pre-saturation (Figure 5.27), so the initially fast dissipation rate might be related to the formation of bleed channels. Furthermore, this may imply that an initially fast bleeding rate is less desirable. Consequently, a less saturated mix may help to reduce the bleeding effect, but it should be noted that water absorption influences the workability and strength of concrete [5].

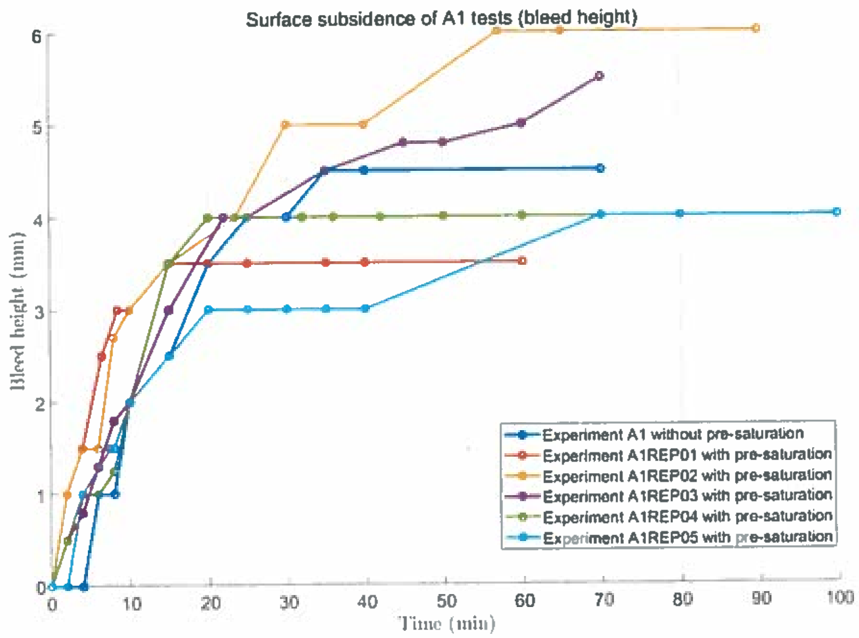

Figure 5.17: Surface subsidence (bleed height) of A1 tests

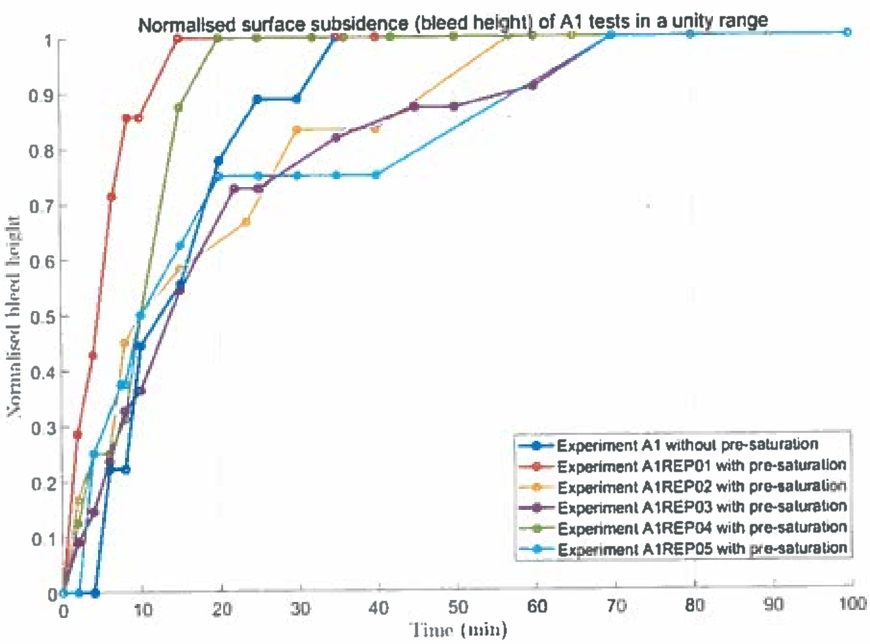

Figure 5.18: Normalised surface subsidence (bleed height) of A1 tests

Since the A1REP04 sample (the fourth repetition of the A1 reference mix) lay in the middle of the five repetitions of the A1 reference mix with pre-saturation (Figure 5.20), A1REP04 was chosen to be compared with the site test data. It can be seen that the pre-saturated A1 reference mix faithfully reproduced the bleeding behaviour of the tremie concrete used on site (Figure 5.16).

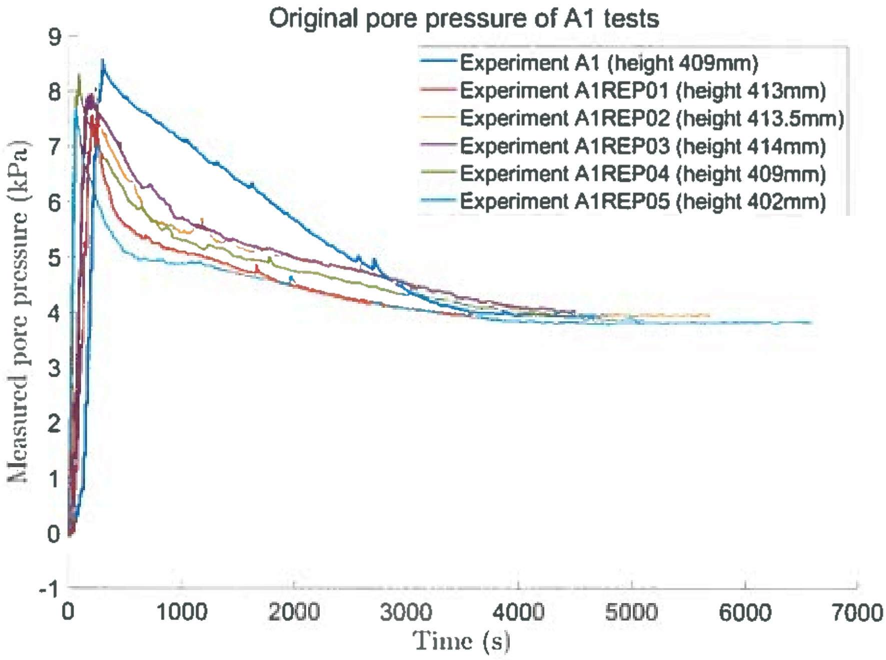

Figure 5.19: Original bottom pore pressure variation of A1 tests

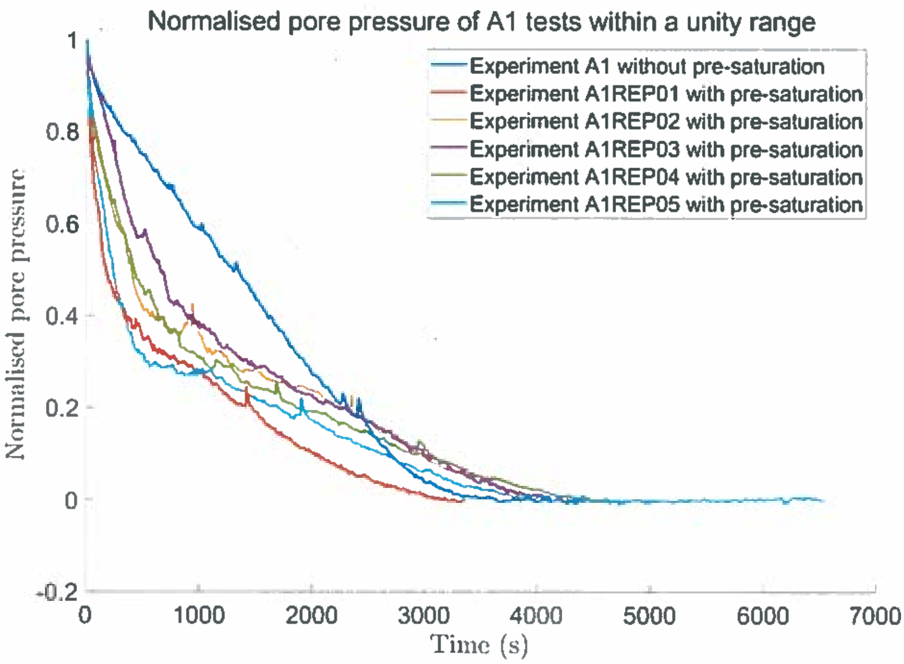

Figure 5.20: Normalised bottom pore pressure variation of A1 tests

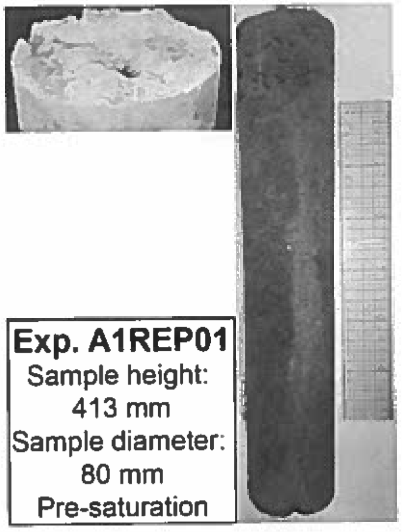

Figure 5.21: Experiment A1REP01

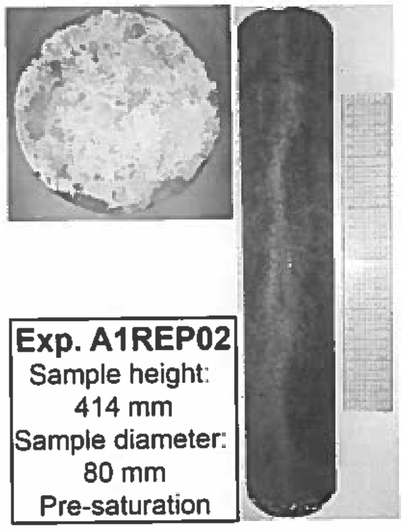

Figure 5.22: Experiment A1REP02

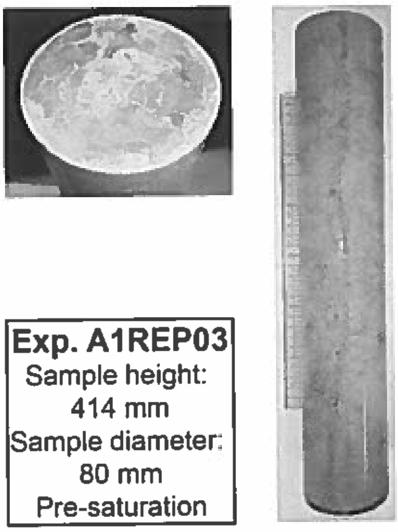

Figure 5.23: Experiment A1REP03

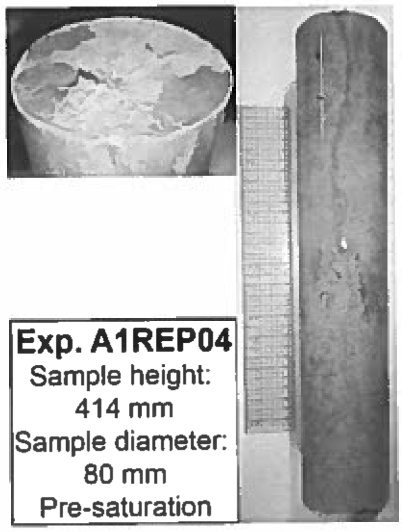

Figure 5.24: Experiment A1REP04

Figure 5.25: Experiment A1REP05

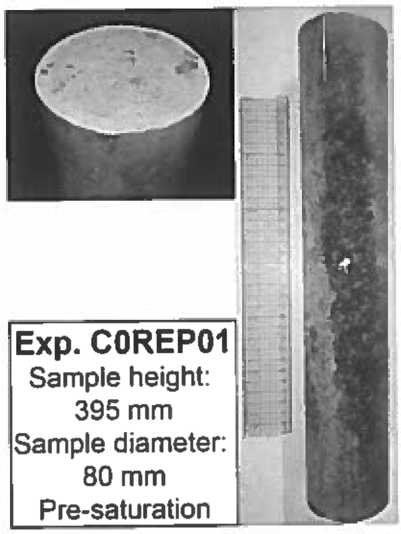

Figure 5.26: Experiment COREP01

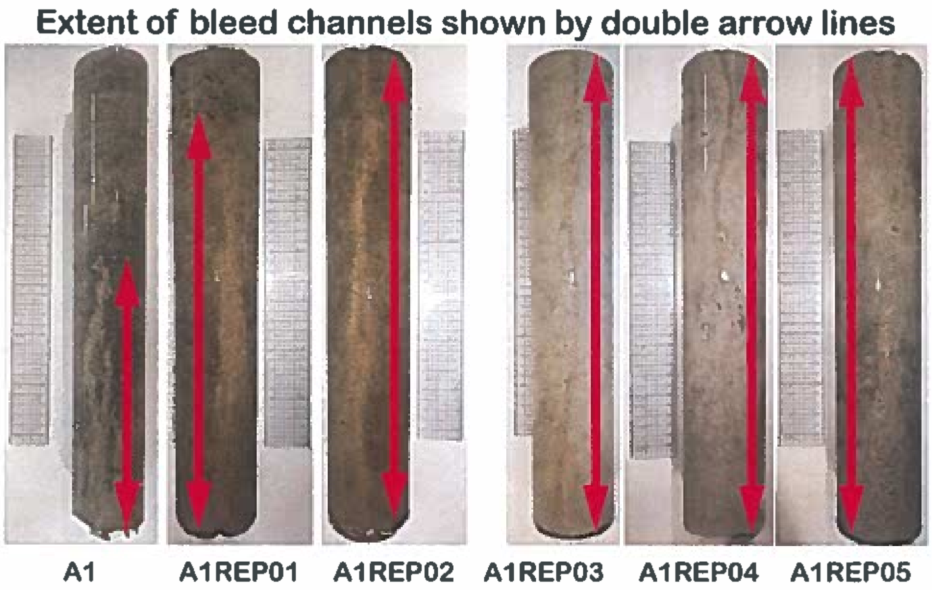

Figure 5.27: Comparison of channelling effect of A1experiments (A1: no pre-saturation; A1REP01 to A1REP05: with pre-saturation)

5.3 Validity of the Proposed Model

The proposed one-dimensional self-weight consolidation model represented by Equation (3.17) was examined using the repeated A1 experimental results by fitting curves of theoretical solution for the experimental data. Based on the work of Picandet et al. [21], the C_v values were chosen to be of the order of 10^{-6} m^2/s. Plots of the experimental data and theoretical results are shown in Figures 5.28 to 5.30.

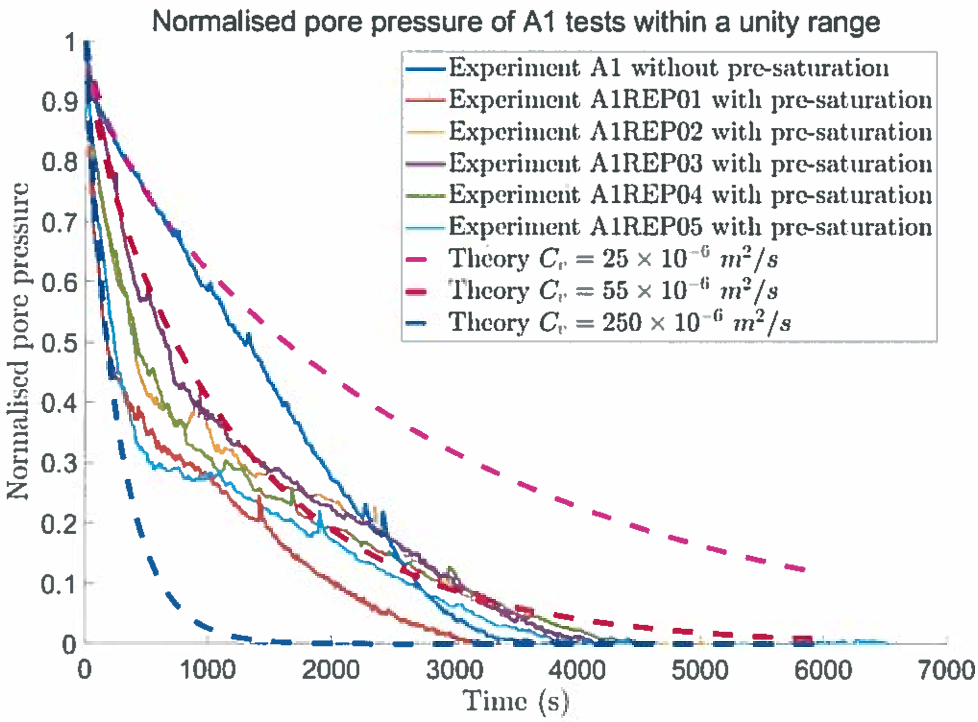

Figure 5.28: Theoretical solutions compared with A1 tests over two hours

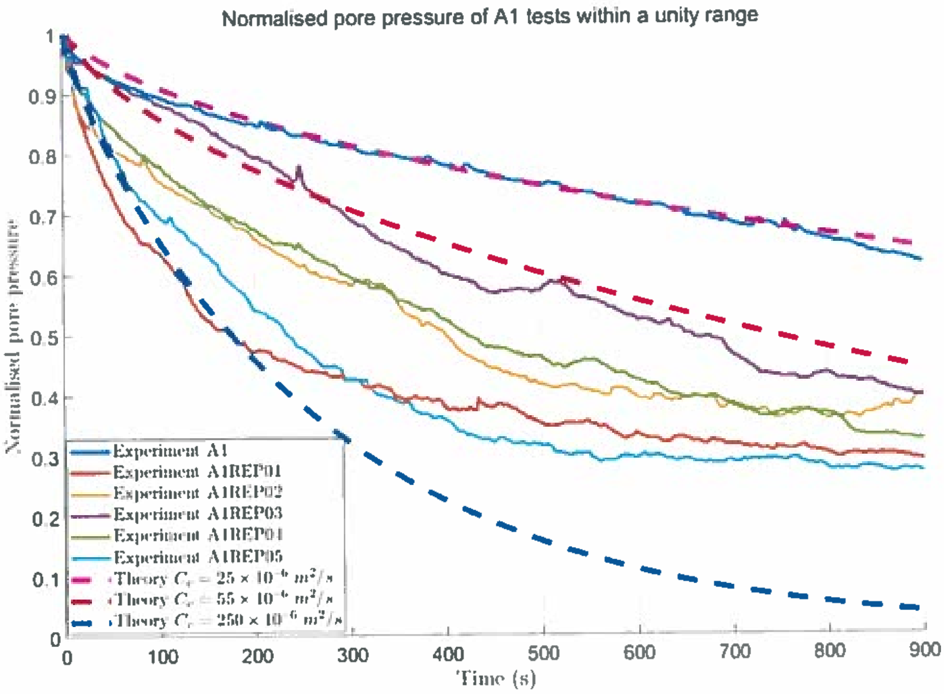

Figure 5.29: Theoretical solutions compared with normalised A1 tests over the first 15 minutes

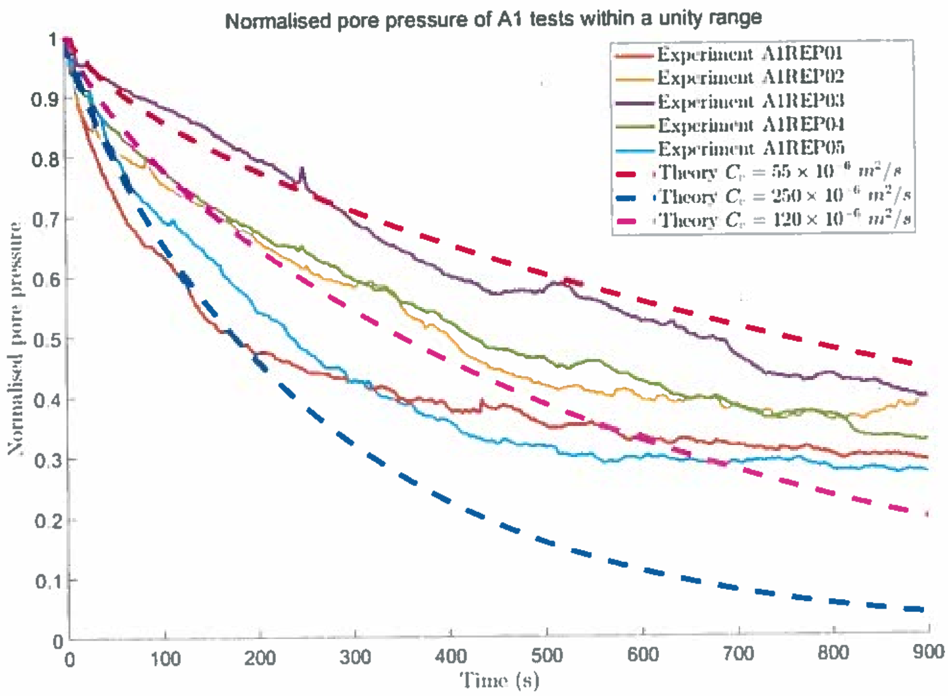

Figure 5.30: Theoretical solutions compared with normalised pre-saturated A1 tests over the first 15 minutes

For the entire two-hour period (Figure 5.28), the one-dimensional self-weight consolidation solutions do not consistently follow all A1 experiments. Excluding the initial A1 test (without pre-saturation), a value of $C_v = 55 \times 10^{-6}\ m^2/s$ probably characterised the A1 reference mix and, hence, the tremie concrete used in site tests. Nevertheless, this value was best regarded as a lower limit of the theoretical solutions for the A1 experiment. The upper limit of the fitted theoretical curve was $C_v = 250 \times 10^{-6}\ m^2/s$ for the first 3 minutes (180 seconds). All pre-saturated A1 data shift towards the curve of $C_v = 55 \times 10^{-6}\ m^2/s$ after about 15 minutes (900 seconds). This was a desirable effect as a reduction in the pore pressure dissipation rate indicated a decrease in the bleeding rate (Equations (2.7), (3.1) and (3.19)) and less severe bleeding effect [2].

Furthermore, some experimental results from Tan et al. [10] also show inconsistencies with the theoretical results, but they were deliberately neglected as the experiment time was limited to 30 minutes. Two of their results are shown in Figure 5.31 for comparison. However, as stated by Tan et al. [10], the consolidation mechanism is probably not the dominant process after a certain time, since the bleed water begins to be absorbed by the hydration and setting of concrete. As a result, the A1 experimental results were also compared with the theoretical solution only for the first 15 minutes so that there was less disturbance to the consolidation process. 15 minutes is also a reasonably short period for the site test.

Figures 5.29 and 5.30 show that the spread of A1 repetitions is still as significant as it is during the entire two-hour period. Nevertheless, experimental results of A1 and A1REFP03 are close to the theoretical expectations. $C_v = 120 \times 10^{-6}\ m^2/s$ may be a better representation of all five repetitions for the first 15 minutes (Figure 5.30).

The discrepancy between the theoretical and the experimental results may not just indicate that the proposed model is incorrect. As shown in Figure 5.36 in the Section 5.4, there can be a theoretical solution closer to each experimental data over the first 15 minutes when every single experimental result was examined separately. Therefore, there might be problems with the prepared tremie concrete (A1REP01 to A1REP05). Inconsistent tremie concrete then resulted in non-uniform repeated data. As discussed further in the last section, although different methods were applied to increase the accuracy of the PPC apparatus, the preparation stage of tremie concrete could introduce a significant inaccuracy into the experimental results. In addition to the revision of the one-dimensional self-weight consolidation model, there should be an improvement on the preparation procedures of the laboratory tremie concrete, along with other tests to confirm the consistency of the produced tremie concrete.

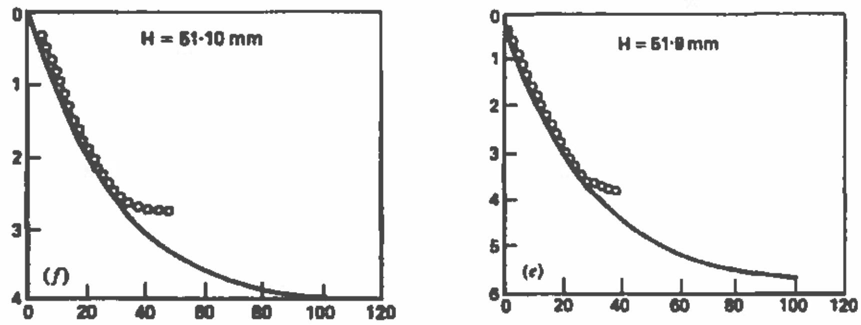

Figure 5.31: Two plots (with surface subsidence in mm against time in minute and sample height H in mm) from the study of Tan et al. (dots: experimental data; lines: theoretical solutions) [10]

Furthermore, it was found that more attention should be paid to the initial bleeding rate compared with the final bleeding capacity. Since the water-binder ratio was designed to fully hydrate and cure the concrete structure in order to achieve the designed properties, the total bleed water should be eventually consumed by various reactions in the surrounding tremie concrete [1, 3, 5, 28]. If the initial bleeding rate can be kept low, the bleeding effect should become negligible as the bleed water is absorbed by following concrete reactions. The stronger channelling effect in samples A1REP01 to A1REP05 (Figure 5.27) of higher initial bleeding rates may also show that a good control of the initial bleeding rate may reduce the overall bleeding. It can also be concluded that it may not be a good decision to control bleeding by simply changing the water content, as many key properties (including strength) of the structure are designed by the water-binder ratio [1, 5, 28].

The deviation of the experimental data from the theorical prediction happens around 20 minutes for traditional cement paste used by Tan et al. [10] (Figure 5.31), and it happened similarly around 15 minutes for modern tremie concrete in this project(Figure 5.28). If the assumption (limiting the time for the examination of bleeding mechanism) from Tan et al. [10] is correct, it may also be concluded that the application of the superplasticiser did not slow down all concrete reactions, but only increased the workability. This may agree with the experimental data of the B1 mix design in the preliminary tests as the negative absorption took place immediately after the preparation stage. Nevertheless, one improvement from the PPC test and the one-dimensional self-weight consolidation model was that a range of bleeding rates could be inferred for a certain type of tremie concrete from Equations (3.19). Although the proposed theory did not fully align with the experimental pore pressure dissipation curves, it is still better to have a range of bleeding rate for a certain type of tremie concrete rather than a single average bleeding rate for all types of tremie concrete. The coefficient of permeability (K) can be found by the apparatus descried by Picandet et al. [21] or from the BAUER test [24]. With a suitable choice of E_0' and the found range for C_v, the bleeding rate as a function of time can be deduced and provided to the construction industry. A better way involves replacing the conventional bleeding site test with the more robust PPC test and directly limiting the C_v values.

5.4 Specific Surface Area Tests

Further experiments were carried out to investigate the effect of specific surface area on bleeding by changing the amount of fine sand, as the previous section shows that changing the water content may not be the most effective strategy to control bleeding. Since fine sand has a greater specific surface area than coarse aggregate, a (proper) increase in the amount of fine sand should increase the specific surface area of tremie concrete. The amount of fine sand in the D0 mix design was 10% (in the fine sand-aggregate ratio by weight) less than the A1 reference mix design (Table 4.1), so the specific surface area of the D0 mix design was less than that of the A1 reference mix design. On the contrary, the D1 mix design was 10% greater in the amount of fine sand, therefore, it had a greater specific surface area than the A1 reference mix design.

Meanwhile, experiments A2 (a pure cement paste) and A3 (a cement paste with sand) were also performed to compare with the results reported in a recent study of modern cement pastes from Peng et al. [12], as mentioned in Chapter 2. Both mixes (A2 and A3) were designed with the same total mass, and water- and superplasticiser-binder ratios as the A1 reference mix design; the sand-binder ratio was also the same for the A3 mix design (Table 4.1). Since A2 and A3 mixes are similar to the A1 reference mix design, experimental results of A2 and A3 were also compared in the specific surface area tests. As the A2 mix only containd binder (the finest constituent in the A1 reference mix design) and the A3 mix design had no gravels, the A2 mix design had the greatest specific surface area following by the A3 mix design among the total five (A1, A2, A3, D0, D1) mix designs in the specific surface area tests. Figures 5.32 to 5.34 show the experimental results, and theoretical solutions of the proposed model are plotted in Figures 5.35 and 5.36.

Figure 5.32 indicates how the decrease in the specific surface area increased the pore pressure dissipation rate and, thus, bleeding rate. This agreed with the suggestions from previous studies [2, 3]. The D1 results, however, need to be reproduced, as the 10% increase in the amount of fine sand was probably still within the range of variation for the A1 reference mix design.

Experimental results of A2 and A3 were almost straight lines (Figure 5.32), so they are similar to the results reported by Peng et al. [12] but not to the plot from Radocea (Figure 2.8) [16]. Peng et al. [12] suggest that the constant bleeding rate may be caused by the addition of plasticiser, and superplasticiser was, in fact, used in this project. However, including A2 and A3 plots, none of the experimental results from this project showed an initial convex shape as shown in Figure 2.8. This difference questions how Peng et al. [12] proved the validity of the plot from Radocea [16], as there is also only a single plot in their research showing the similar shape to the plot in Figure 2.8. Nevertheless, the deviation of the experimental results from the Radocea's plot may indicate the difference between the modern cement-based materials and traditional cement-based materials.

For the first 15 minutes, the theoretical prediction were closer to the experimental results from specific surface area tests (Figure 5.36) than the data from the repeated A1 tests (Figure 5.30). Similar to the normalised surface subsidence plots in previous sections (Figures 5.4 and 5.18), the order of change in bleeding rates of the normalised surface subsidence plot in the specific surface area tests (Figure 5.34) was approximately in line with the order of pore pressure dissipation rates of the normalised excess pore pressure plot (Figure 5.32), but the normalised excess pore pressure plot represented a clearer difference among different experiments. The comparison among the three plots from Figures 5.32 to 5.34 indicated that the normalised method chosen in the data analysis did not provide any information about the bleeding capacity. Nonetheless, as discussed in the previous section, more attention should be paid to the initial bleeding rate and the bleed water should be re-absorbed at last.

Since the PPC test reflected the severity of bleeding to a certain degree over the first 15 minutes, the 15-minute PPC test may be performed in the factory before the tremie concrete is transported to site. This can help reduce the costs from transporting and dumping unacceptable tremie concrete (in bleeding). Remixing with fines may help to control the bleeding of tremie concrete, but there must be further research on how the remixing affects other tremie concrete properties [3].

Furthermore, the first issue identified during the specific surface area tests was that the specific surface areas of mix designs C0 and C1 did not change as much as expected by simply changing the amount of fine sand (Figure 5.37). For the C0 mix design, a simple reduction in the amount of fine sand was accompanied by a decrease in the aggregate-binder ratio. As a result, the reduction in fine sand was compensated by the increase in the amount of binder. Mix designs were consequently improved to D0 and D1 by keeping the total mass and aggregate-binder ratio constant, and increasing or decreasing the fine sand-aggregate ratio by 10%. Figure 5.37 shows that there was basically no difference in bleeding among C0REP01 and A1 repeated experiments, but the bleeding was distinct in D0 experiment.

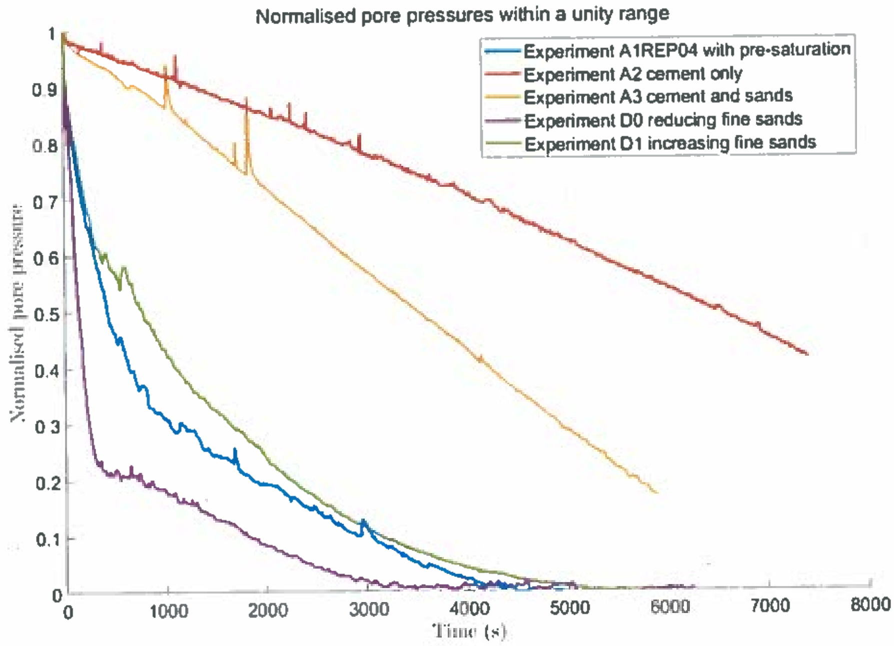

Figure 5.32: Normalised pore pressures used to examine the effect of specific surface area

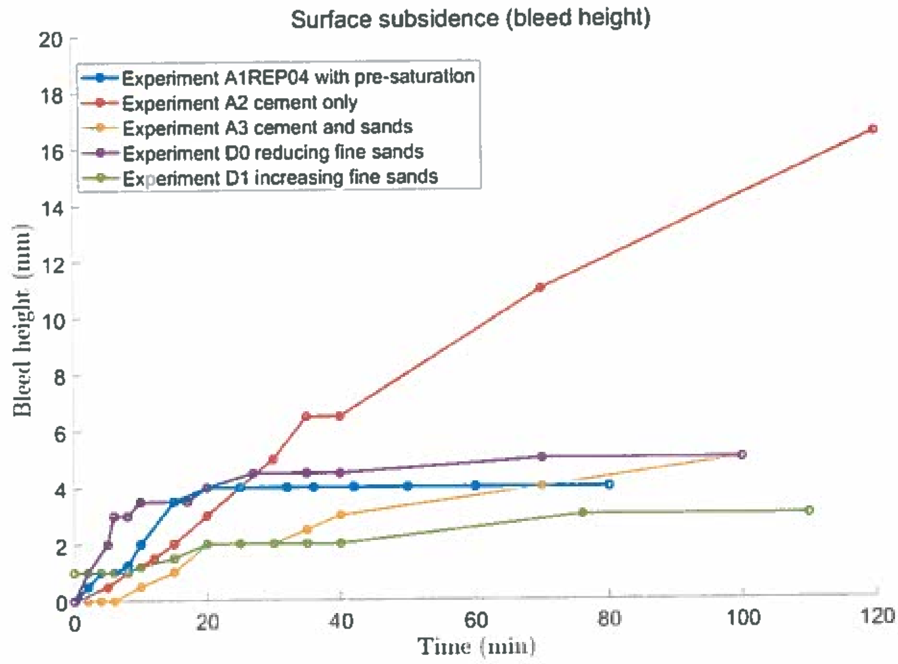

Figure 5.33: Surface subsidence used to examine the effect of specific surface area

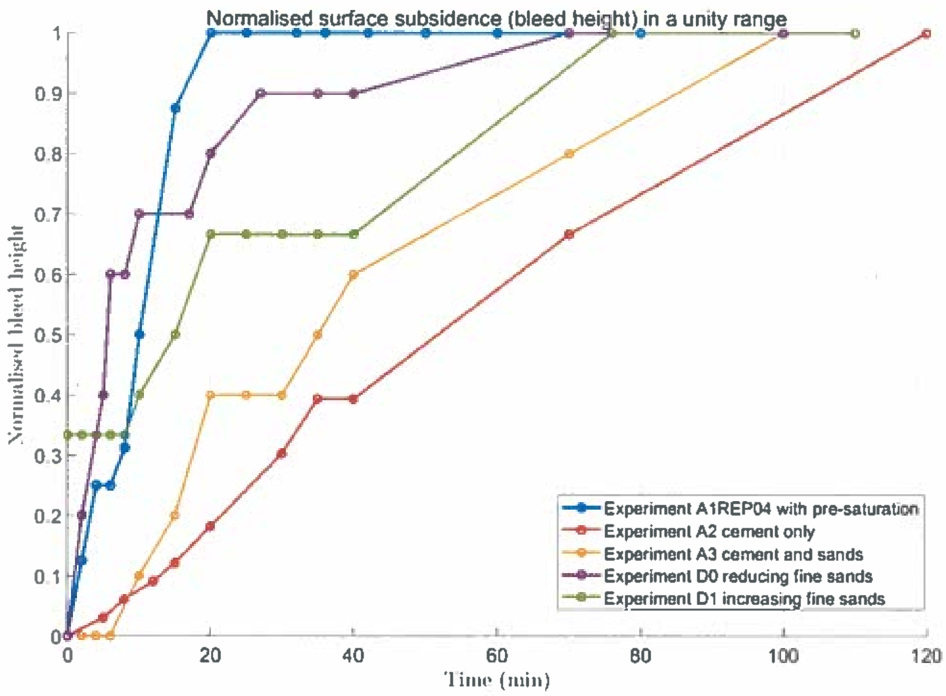

Figure 5.34: Normalised surface subsidence used to examine the effect of specific surface area

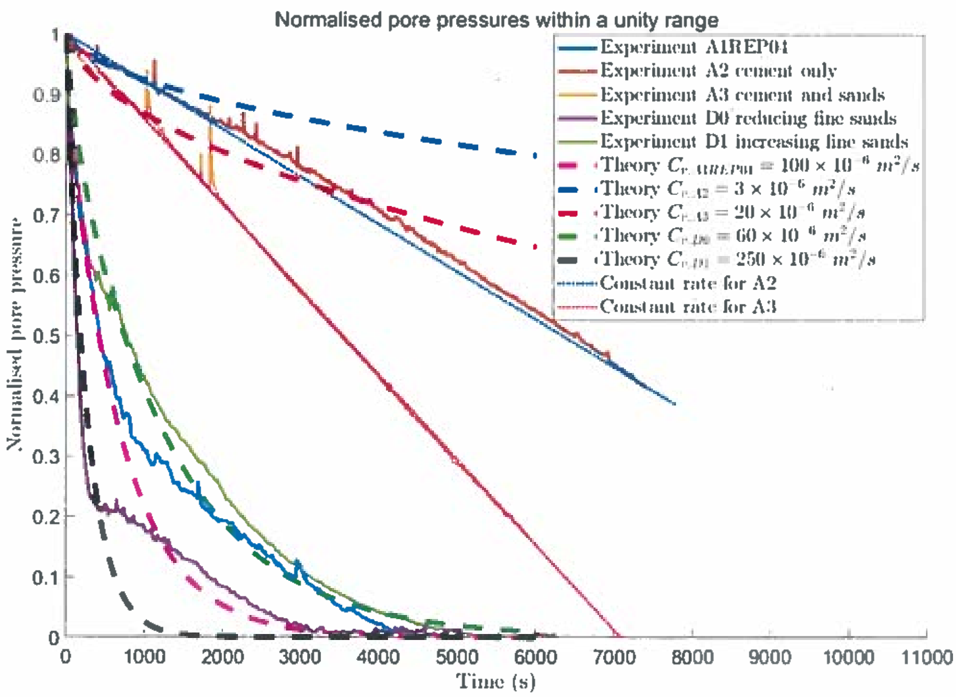

Figure 5.35: Proposed theory compared to normalised pore pressure over the first two hours to examine the effect of specific surface area

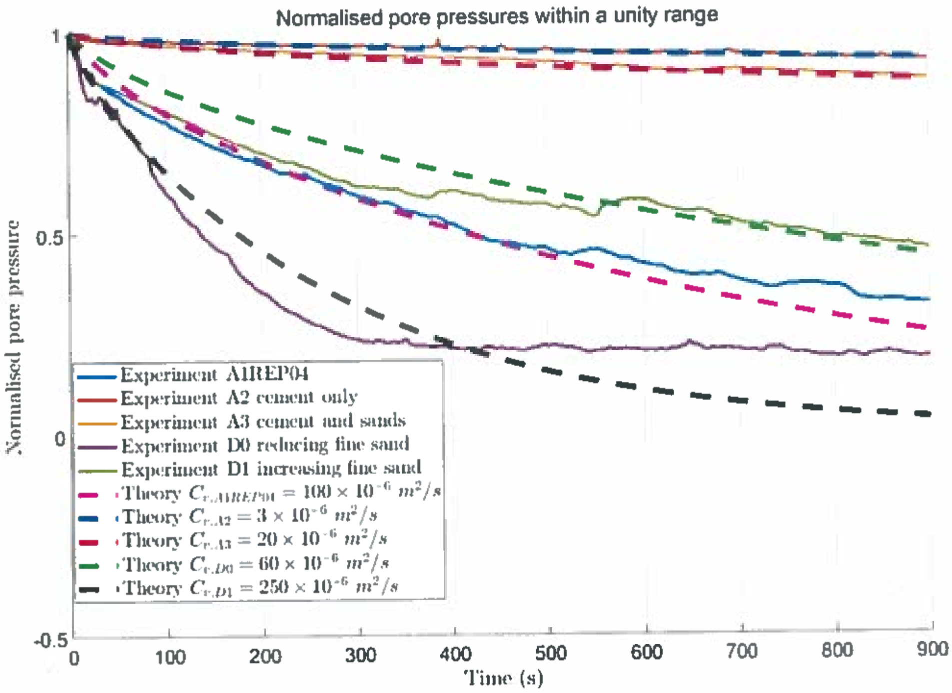

Figure 5.36: Proposed theory compared to normalised pore pressure over the first 15 minutes to examine the effect of specific surface area

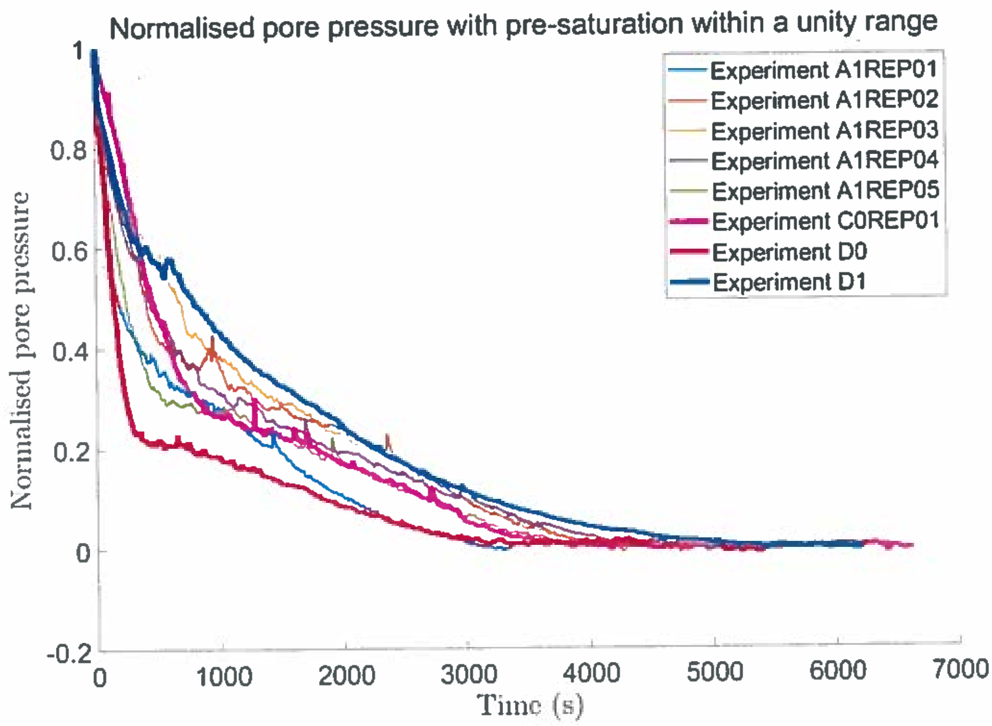

Figure 5.37: Normalised pore pressures used in the comparison with the C0 and D0 mixes

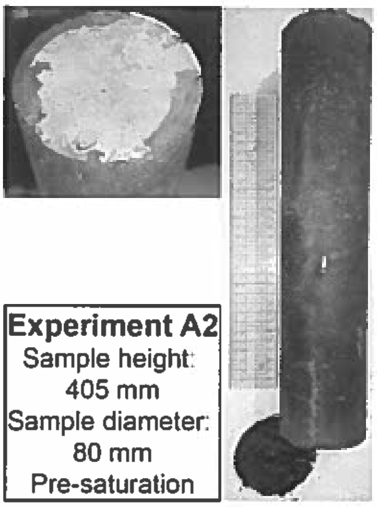

Figure 5.38: Experiment A2

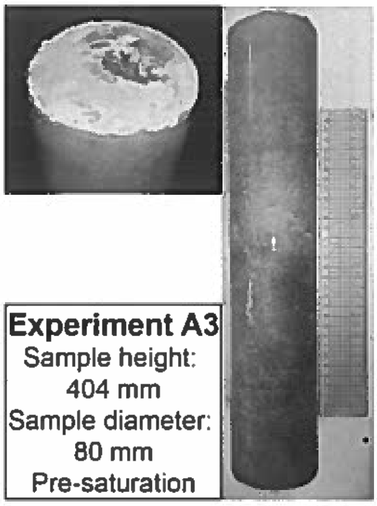

Figure 5.39: Experiment A3

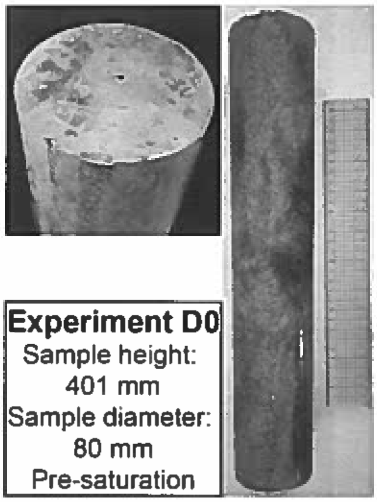

Figure 5.40: Experiment D0

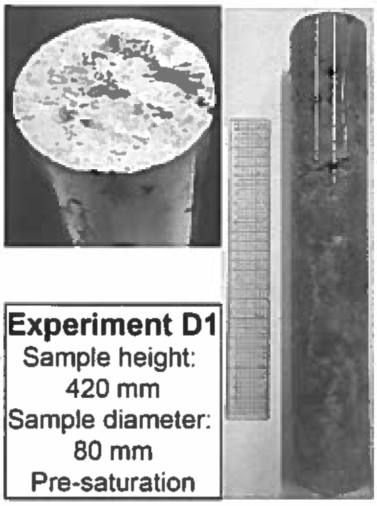

Figure 5.41: Experiment D1

5.5 Remarks on the PPC Test

Figure 5.42 shows that there was more than 180 seconds (3 minutes) reduction in the tremie concrete placement by the use of a special funnel (Figure 4.4). A faster tremie concrete placement reduced the amount of small consolidation after each scoop of tremie concrete was placed, as shown by the small dip after each increment in pressure. For future studies on bleeding, a miniature replica of hopper and tremie pipe (used on site) can be designed to fit in the PPC test, so the tremie concrete placement will be performed in close proximity to the real situation. In contrast to the rough condition inside the tremie concrete sample, the smooth cylinder wall had much less resistance to the formation of bleed channels and, hence, it encouraged the formation of surface bleed channels. The transparent cylinder wall also allowed for the observation of surface bleed channels. The extent of surface bleed channels was used for the preliminary qualification of the severity of bleeding.

Apart from adding a special funnel to reduce placing time, there were other attempts to improve the accuracy of the PPC test, such as recording the initial pore pressure, fixing a scale for surface subsidence reading, using a timber support to level the cylinder and using a foam to minimise noise. In contrast to the current site test on bleeding, the PPC test is more robust and can clearly compare the bleeding behaviour for first 10 to 15 minutes. This indicates an opportunity for the future application of the PPC test on site.

However, as mentioned in Section 5.3, the preparation of tremie concrete might introduce considerable inaccuracy into experimental results and, hence, affected the investigation of the proposed bleeding mechanism. First, there was a less precise control of the pre-saturation and mixing time, since there was no independent check on time. Second, the pre-saturation stage did not produce the ideal saturated and surface-dry aggregate, as there was no procedure to confirm the degree of saturation, and it influenced the actual water content in laboratory tremie concrete [5, 11, 15, 28]. Thirdly, a non-standard mixing device was used due to the small amount of tremie concrete required. The handheld stirring device for the mixing of the tremie concrete could not maintain a consistent rotation rate, and mixing in a bucket could influence the homogeneity of the tremie concrete compared with what were done in other research [12, 15]. Finally, for the A1 repetitions, there was no parallel standard tests (such as slump-flow and cube strength tests) to check the uniformity of repetitions [1, 15].

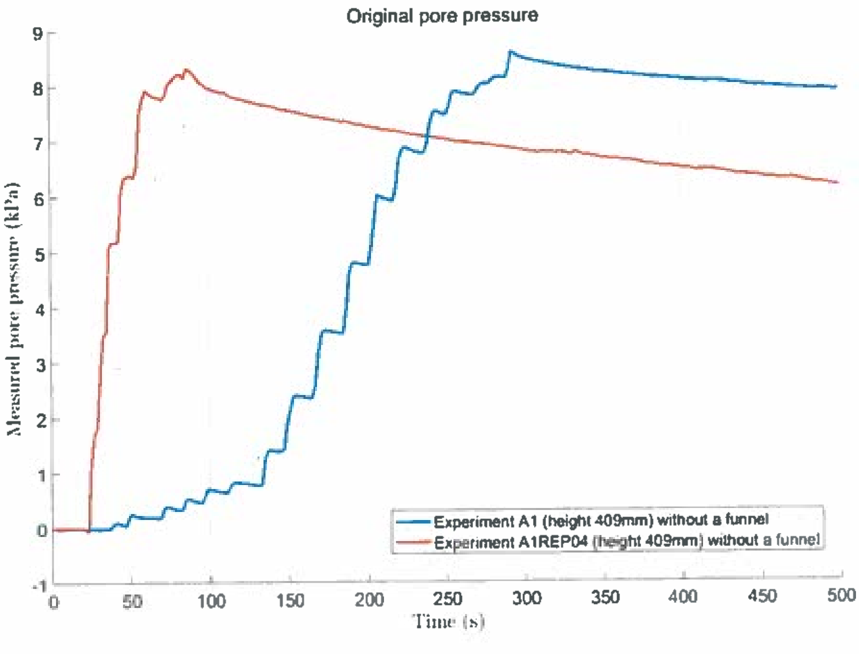

Figure 5.42: Time reduction using a special funnel

For future repetitions of the PPC test, there should be an independent and more precise control on the time. Instead of a simple pre-saturation stage, there should be an improvement to produce the saturated and surface-dry aggregate. Moreover, a larger amount of tremie concrete can be produced by a standard mixer for future experiments, so that parallel standard tests can be performed together with the PPC test. Nonetheless, as the PPC test is potentially applicable on site, the future PPC tests probably can be directly performed on site with proper construction tremie concrete. Then, there should be less concern about the quality of tremie concrete.

The severity of bleeding was not qualitatively studied by the PPC test, and there is still not a good way to identify bleeding alone. Nevertheless, since the qualitative classification of bleeding aimed to provide a range of bleeding rates (or other relevant parameters) for the acceptable bleeding, this range can be alternatively produced by repetitions of the PPC test with a standard mix design. For example, in terms of the A1 reference mix used in this project, a range of C_v values (such as 55 to 200 $\times 10^{-6}$ m^2/s) from the PPC test may be used to limit the acceptable bleeding of the A1 reference mix for its later application in construction. Moreover, changing the specific surface area can be a good choice for the future PPC tests to qualify bleeding.

6 Conclusions

This project was proposed to analyse the bleeding behaviour of tremie concrete following the study of bleeding problems in deep foundations and current site tests. From the literature review, the one-dimensional self-weight consolidation was suggested as the mechanism underlying the bleeding of tremie concrete. Theoretical solutions (of the excess pore pressure, surface subsidence and bleeding rate) were consequently deduced based on Terzaghi's equation, and the PPC test was developed to confirm the proposed model by comparing the experimental measurement of pore pressure with the theoretical solution. A noteworthy advantage of the proposed one-dimensional self-weight consolidation model was that only a single variable C_v is involved in the theoretical solution of the excess pore pressure.

The preliminary tests were first performed to validate the feasibility of the PPC test. Recognisable curves (with shapes close to expectations) of the A1 reference mix design and five other extreme cases of bleeding were produced by the PPC test. The experimental procedure was proved to be repeatable, and the PPC test was found to be accurate and less susceptible to human error. Therefore, the PPC test was used for the examination of the proposed consolidation model.

The PPC test was also performed on-site to investigate its potential for site applications and to compare laboratory tremie concrete with tremie concrete used in real construction. Although there was noticeable noise from the surroundings on site, the PPC test was still able to analyse the bleeding effect. Moreover, the site experience highlighted the need for a pre-saturation step in the preparation of laboratory tremie concrete. This step was then added to all following experiments, so the bleeding behaviour of laboratory tremie concrete was similar to that of construction tremie concrete. It was also found that dry aggregate actually performed better in resisting bleeding as it had a much slower bleeding rate, although this had potential negative effects on other properties of tremie concrete.

The derived one-dimensional self-weight consolidation model was compared with the results from the repeated experiments of the A1 reference mix design and the specific surface area tests. Due to the spread of the A1 repetition results, the validity of the propose model was uncertain and further work is required. Nevertheless, it can be seen that, after a certain time, there was a general trend of decrease in C_v values and, thus, the bleeding rate, since the water-absorption from the hydration and setting of tremie concrete might begin to dominate the process. This was a desirable effect, and it may imply that the initial bleeding rate mainly determines the severity of bleeding. Together with observations from cured samples (A1 to A1REP05), it can be concluded that a decrease in the initial bleeding rate can reduce the overall bleeding.

As other reactions (hydration and setting) might dominate in tremie concrete after a certain time, the experimental data were chosen to be further compared with the proposed model within the first 15 minutes. The deviation from the theoretical solution was still considerable, but it was more significant in the A1 repeated data than in the specific surface area experimental results. Consequently, there was a concern that inaccuracy from the preparation of laboratory tremie concrete largely influenced the interpretation of the proposed model. There was also a lack of standard tests to check the uniformity of the repetitions of the A1 reference mix design and the pre-saturation and mixing stages were probably not precisely controlled. As many methods were applied to the PPC test to maintain a high accuracy, further repetitions should focus on producing consistent tremie concrete in the laboratory.

In the specific surface area tests, results from the cement paste (A2 and A3 experiments) were in line with the previous research from Peng et al. [12] but not with the research from Radocea [16], so this probably showed the difference between modern cement-based materials and traditional ones used in the earlier research. The increase in the specific surface area clearly reduced in the bleeding rate. Therefore, Powers' argument about the bleeding rate which depends on the balance between the particle's self-weight (proportional to the particle's volume) and the viscous drag around the particle (proportional to the particle's surface area) is still applicable to modern tremie concrete. Further research can use different amounts of fine sand to qualitatively control the severity of tremie concrete bleeding, and then provide a range of acceptable bleeding rates for a certain type of tremie concrete.

In contrast to the single upper limit of an average bleeding rate used for all types of tremie concrete in current site tests, the robust PPC test can at least provide an acceptable range of bleeding rates for a certain type of tremie concrete based on repetitions of the standard mix design. Accordingly, repetitions will show a range of bleeding rates that the standard mix design of a certain type of tremie concrete can vary due to human error, temperature change and other possible inaccuracies. A direct limit on that produced range of bleeding rates can provide a baseline for bleeding of a certain type of tremie concrete regardless of the qualification of bleeding. Nevertheless, this is an inefficient approach involving heavy work.

Since the PPC test clearly distinguished different types of tremie concrete within the first 15 minutes, it can be used on site in the future for a short (15-minute) test to replace the current long and manual one. Furthermore, for the future application of the PPC test on site, there can be a limit on the pore pressure dissipation rates or the C_v values instead of converting the measurements into bleeding rates.

References

[1] EFFC/DFI Concrete Task Group, "Guide to Tremie Concrete for Deep Foundations (second edition)," 2018.

[2] T. C. Powers, "Properties of Fresh Concrete," *Wiley, New York*, 1968.

[3] J. F. Lamond and J. H. Pielert, "Significance of Tests and Materials and Concrete-Making Properties of Concrete STP 169D," *ASTM International*, 2006.

[4] A. Thorp, C. Wilkes, D. Nicholson, and B. Marsh, "Recent experience of tremie concrete properties and testing," *DFI-EFFC International Conference on Deep Foundations and Ground Improvement, Rome*, 2018.

[5] J.J.Brook and A.M.Nevillie, "Concrete Technology (Second Edition)," *Pearson Education Ltd., UK*, 2010.

[6] The Aberdeen Group, "Concrete bleeding Causes, effects and control," 1988.

[7] American Society for Testing Materials (ASTM) International, "C232/C232M-12: Standard Test Methods for Bleeding of Concrete," *ASTM Standards*, 2012.

[8] British Standards Institution (BSI), "BS EN 480-4:2005 Admixtures for concrete, mortar and grout — Test methods — Part 4: Determination of bleeding of concrete," *British Standards*, vol. 3, 1997.

[9] A. Radocea, "A new method for studying bleeding of cement paste," *Cement and Concrete Research*, vol. 22, no. 5, pp. 855–868, 1992.

[10] T. S. Tan, T. H. Wee, S. A. Tan, C. T. Tam, and S. L. Lee, "A consolidation model for bleeding of cement paste," *Advances in Cement Research*, vol. 1, no. 1, pp. 18–26, 1987.

[11] H. J. Yim, J. H. Kim, and H. G. Kwak, "Experimental simulation of bleeding under a high concrete column," *Cement and Concrete Research*, vol. 57, pp. 61–69, 2014.

[12] Y. Peng, R. A. Lauten, K. Reknes, and S. Jacobsen, "Bleeding and sedimentation of cement paste measured by hydrostatic pressure and Turbiscan," *Cement and Concrete Composites*, vol. 76, pp. 25–38, 2017.

[13] A. Draganovic, "Bleeding and Filtration of Cement - Based Grout," *KTH Architecture and the Built Environment*, 2009.

[14] N. Massoussi, E. Keita, and N. Roussel, "The heterogeneous nature of bleeding in cement pastes," *Cement and Concrete Research*, vol. 95, pp. 108–116, 2017.

[15] H. J. Yim, J. H. Kim, H. G. Kwak, and J. K. Kim, "Evaluation of internal bleeding in concrete using a self-weight bleeding test," *Cement and Concrete Research*, vol. 53, pp. 18–24, 2013.

[16] A. Radocea, "A model of plastic shrinkage," *Magazine of Concrete Research*, vol. 46, no. 167, pp. 125–132, 1994.

[17] H. Steinour, "Further Studies of The Bleeding of Portland Cement Paste," *Portland Cement Assotiation*, pp. 1–108, 1945.

[18] Y. Peng and S. Jacobsen, "Influence of water/cement ratio, admixtures and filler on sedimentation and bleeding of cement paste," *Cement and Concrete Research*, vol. 54, pp. 133–142, 2013.

[19] L. Josserand, O. Coussy, and F. de Larrard, "Bleeding of concrete as an ageing consolidation process," *Cement and Concrete Research*, vol. 36, no. 9, pp. 1603–1608, 2006.

[20] American Society for Testing Materials (ASTM) International, "ASTM C232/C232M-14: Standard Test Method for Bleeding of Concrete," *ASTM Standards*, pp. 1–5, 2014.

[21] V. Picandet, D. Rangeard, A. Perrot, and T. Lecompte, "Permeability measurement of fresh cement paste," *Cement and Concrete Research*, vol. 41, no. 3, pp. 330–338, 2011.

[22] A. Perrot, D. Rangeard, V. Picandet, and Y. Mélinge, "Hydro-mechanical properties of fresh cement pastes containing polycarboxylate superplasticizer," *Cement and Concrete Research*, vol. 53, pp. 221–228, 2013.

[23] L Josser and F de Larrard, L. Josserand, and F. De Larrard, "A method for concrete bleeding measurement," *Materials and Structures*, vol. 37, no. 274, pp. 666–670, 2004.

[24] BAUER Group, "Operating instructions BAUER Concrete filter press," *Company Management Manual BAUER Group*, pp. 1–9, 2015.

[25] Y. Ji, Z. Sun, X. Yang, C. Li, and X. Tang, "Assessment and mechanism study of bleeding process in cement paste by 1H low-field NMR," *Construction and Building Materials*, vol. 100, pp. 255–261, 2015.

[26] ACI Committee 211, "Standard Practice for Selecting Proportions for Normal Heavyweight, and Mass Concrete (ACI 211. 1-91) Reapproved 1997," *ACI Committee Reports*, pp. 1–38, 2002.

[27] J. García-González, D. Rodríguez-Robles, A. Juan-Valdés, J. M. del Pozo, and M. I. Guerra-Romero, "Pre-saturation technique of the recycled aggregates: Solution to the water absorption drawback in the recycled concrete manufacture," *Materials*, vol. 7, no. 9, pp. 6224–6236, 2014.

[28] BIBM, EFCA, ERMCO, EFNARC, and CEMBUREAU, "The European Guidelines for Self-Compacting Concrete Specification, Production and Use," 2005.

[29] R. D. Holtz, W. D. Kovacs, and C. S. Sheahan, "An Introduction to Geotechnical Engineering (second edition)," *Pearson, Upper Saddle River, NJ*, 2011.

[30] W. Powrie, "Soil mechanics : concepts and applications (second edition)," *London Spon*, 1997.

[31] C. Fierenkothen and M. Pulsfort, "The spreading of fresh concrete in bored piles-results of large and small scale model tests and numerical simulations," *ICSMGE 2017 - 19th International Conference on Soil Mechanics and Geotechnical Engineering*, pp. 919–924, 2017.

[32] D. Buglass, "Flow of Tremie Concrete in Deep Foundations," *Department of Engineering University of Cambridge*, 2018.

[33] G. F. Kheder and R. S. Al Jadiri, "New method for proportioning self-consolidating concrete based on compressive strength requirements," *ACI Materials Journal*, vol. 107, no. 5, pp. 490–497, 2010.

A Risk Assessment Retrospective

Overall, this project was carried out at a high Health and Safety standard though it actually involved several high-risk activities, including the use of Control of Substances Hazardous to Health (COSHH) constituents of concrete, electric-powered tools and the power supply. The completion of a thorough risk assessment document from the Engineering Department, acquisition of the Project Approval Document (PAD) from the Schofield Centre, as well as suggestions from the supervisor, PhD student and technicians are proved to be extremely helpful.

The project was executed without any issues, emergencies or overtime challenges, however, there was little experience with the newly designed PPC test. As the documentation requirements slowed down the rush towards the practical phase at the beginning of this project, several weeks were spent to consolidate the limited previous experience with the PPC test. As a result, each experiment was planned at least a week ahead during weekly meetings, and each new experimental method was properly demonstrated and supervised by technicians before being added to the experimental procedure. Therefore, even minor problems which could have arose from missing or misunderstanding steps were avoided.

Nonetheless, the complexity of two experimental procedures (mixing tremie concrete and taking out cured sample) were underestimated and they were not dealt with properly in the risk assessment documents. Extra time was spent on working out solutions to these challenges. For the preparation of the tremie concrete, a specially designed stirring tool was used to mix the small amount of tremie concrete. The handheld stirring tool exposed the user to different risks compared to the standard mixer. Nevertheless, the use of the tool was first demonstrated and supervised by the technician and then potential hazards were discussed. Furthermore, there was not a carefully planned step about taking out the cured sample from the apparatus. It was then decided that compressed air should be used; a process which was also properly demonstrated and supervised. Although there were such unexpected issues, the Health and Safety precautions developed from the risk assessment procedure provided a good reference for the later uncertainties.

If this project were to start again, it may be prudent to go through the practical experiment step-by-step with the supervisor and technicians for the risk assessment. Their experience is more practically helpful, and they can spot any key missing steps or correlated devices more easily. Moreover, it would be a good idea to ensure that tools are available for use in the laboratory, and that the existence of better tools for the project than what is expected are explored. It is also equally important that there is a more thorough time schedule, leaving enough time to deal with uncertainties and minimising the need to rush during each experiment.